Minnesota State University, Mankato

Cornerstone: A Collection of Scholarly and Creative Works for Minnesota State University, Mankato

All Graduate Theses, Dissertations, and Other Capstone Projects

Graduate Theses, Dissertations, and Other Capstone Projects

2018

Modeling of Small-Scale Wind Power System with Virtual Synchronous Generator

Sahithi Nannapaneni
Minnesota State University, Mankato

Follow this and additional works at: https://cornerstone.lib.mnsu.edu/etds

Part of the Power and Energy Commons

Recommended Citation

Nannapaneni, S. (2018). Modeling of Small-Scale Wind Power System with Virtual Synchronous Generator [Master's thesis, Minnesota State University, Mankato]. Cornerstone: A Collection of Scholarly and Creative Works for Minnesota State University, Mankato. https://cornerstone.lib.mnsu.edu/etds/833/

This Thesis is brought to you for free and open access by the Graduate Theses, Dissertations, and Other Capstone Projects at Cornerstone: A Collection of Scholarly and Creative Works for Minnesota State University, Mankato. It has been accepted for inclusion in All Graduate Theses, Dissertations, and Other Capstone Projects by an authorized administrator of Cornerstone: A Collection of Scholarly and Creative Works for Minnesota State University, Mankato.

MODELING OF SMALL-SCALE WIND POWER SYSTEM WITH VIRTUAL SYNCHRONOUS GENERATOR

By

SAHITHI NANNAPANENI

A Thesis Submitted in Partial Fulfillment of the

Requirements for the Degree of

Master of Science

in

Electrical Engineering

Minnesota State University, Mankato

Mankato, Minnesota

December 2018

November, 2nd 2018

MODELING OF SMALL-SCALE WIND POWER SYSTEM WITH VIRTUAL SYNCHRONOUS GENERATOR

By

SAHITHI NANNAPANENI

This thesis has been examined and approved by the following members of the student's committee.

_____

Dr. Vincent Winstead, Ph.D, P.E

_____

Dr. Han-Way Huang, Ph.D

_____

Dr. Xuanhui Wu, Ph.D

ABSTRACT

MODELING OF SMALL-SCALE WIND POWER SYSTEM WITH VIRTUAL SYNCHRONOUS GENERATOR

Sahithi Nannapaneni

Electrical Engineering
Minnesota State University, Mankato
Mankato, Minnesota
December 2018

Wind power systems are the most commonly used systems for a renewable energy source over the past few decades. Most of the current wind turbines are large scale wind turbines which produce mega watts power. This thesis is prepared to develop a small scale wind turbine with axial flux permanent magnet synchronous generator for regional areas and small commercial industries. This thesis mainly focuses on the Axial Flux PMSG which is a small scale prototype with the characteristics of the large scale wind turbine generator and having a super capacitor embedded in it. The first objective is to create the dynamic wind gust model. The second objective is to study the background of the large scale wind turbine synchronous generator characteristics and to derive the equations to model the AFPMSG. The next objective is to implement the super capacitor model with a controller. The other main objective of this thesis is to design a Virtual Synchronous Generator to emulate the inertia and damping same as the conventional synchronous generator to maintain output power and the frequency stable when there is a change in the load. The model will be tested using the MATLAB-Simulink environment and the results will be discussed.

ACKNOWLEDGEMENT

I would like to express my sincere gratitude to Dr.Vincent Winstead for his immense patience, expert guidance, valuable suggestions and support throughout my thesis and course work.

I would like to thank the entire faculty of the Department of Electrical and Computer Engineering for their support and also for giving me immense knowledge from my course work in this university.

Finally, I must express my very profound gratitude to my parents, to my sister and to my partner for providing me with unfailing support and continuous encouragement throughout my years of study and through the process of researching and writing this thesis. This accomplishment would not have been possible without them. Thank you.

Contents

ABSTRACT ii

ACKNOWLEDGEMENT iii

TABLE OF CONTENTS v

LIST OF FIGURES viii

LIST OF TABLES ix

LIST OF ABBREVATIONS x

1 INTRODUCTION **1**

1.1 Literature Review 4

1.2 Objective 7

1.3 Motivation 7

2 MODELING AND ANALYSIS OF WIND TURBINE SYSTEMS **9**

2.1 Introduction to Wind Turbine Systems 9

2.2 Wind Turbine Modeling 9

2.3 Modeling of Axial Flux Permanent Magnet Synchronous Generator . . 13

2.3.1 Introduction to PMSG 13

2.3.2 Mathematical Model of the AFPMSG 14

3 MODELING OF VIRTUAL SYNCHRONOUS GENERATOR 18

3.1 Introduction 18

3.2 Real Power - Frequency Droop Control 19

3.3 Reactive Power- Voltage Control 21

3.4 VSG Algorithm 22

3.5 Current Control 24

4 MODELING OF THE SUPER CAPACITOR 28

5 SIMULATION RESULTS AND ANALYSIS 31

6 CONCLUSION AND FUTURE WORK 45

6.1 Conclusion 45

6.2 Future Work 46

REFERENCES 47

List of Figures

1.1 Global growth of installed wind power capacity [1] 2

1.2 Installed wind power capacity in US by 2017 [2] 3

1.3 Virtual Synchronous Generator [3] 4

2.1 Simulink model of the wind turbine 12

2.2 Simulink model of the wind gust 12

2.3 Dynamic wind gust. 14

2.4 dq model of the synchronous machine 15

2.5 Equivalent circuit of AFPMSG q-axis and d-axis respectively. 16

2.6 Simulink model of the AFPMSG. 17

3.1 Brief Overview of VSG topology 19

3.2 PF droop characteristics. 20

3.3 Simulink model of the PF droop control. 20

3.4 QV droop characteristics. 21

3.5 Simulink model of the QV droop control. 22

3.6 Equivalent circuit of virtual synchronous generator. 23

3.7 Virtual Generator phasor diagram. 24

3.8 Simulink model of the VSG Algorithm. 25

3.9 Equivalent circuit of the LC filter. 26

3.10 Simulink model of the Current Controller. 27

4.1 Simulink model of Super capacitor control system. 29

4.2 Simulink model of control signals. 29

4.3 Simulink model of super capacitor with control signals connected to inverter. 30

5.1 Overview of the Wind power system without control method. 32

5.2 Step wind speed as input (m/s). 32

5.3 Speed of the rotor (rad/s). 33

5.4 Rotor angle (rad). 33

5.5 Electromagnetic Torque (N.m). 34

5.6 Three phase voltage at the load without VSG control (volts). 34

5.7 Three phase current at the load without VSG control (ampere). 35

5.8 The three phase voltage zoom in graph (volts) 35

5.9 Three phase current zoom in graph (ampere). 36

5.10 Active/Real Power without VSG control (10KWatts). 36

5.11 Reactive power without VSG control (10KVar). 37

5.12 Frequency without VSG control (Hz). 37

5.13 Overview of the Power system with VSG and supercapacitor. 38

5.14 Three phase voltage with VSG (volts). 39

5.15 Three phase current with VSG (ampere). 40

5.16 Frequency with VSG (Hz). 40

5.17 d-axis voltage with VSG (volts). 41

5.18 q-axis voltage with VSG (volts). 41

5.19 d-axis current with VSG (ampere). 42

5.20 q-axis current with VSG (ampere). 42

5.21 V_{abc} sine wave (volts). 43

5.22 I_{abc} sine wave (ampere). 43

5.23 Active/Real power with VSG (10KWatts). 44

5.24 Reactive Power with VSG (10KVar). 44

5.25 Charging and discharging of a capacitor (percentage). 44

List of Tables

2.1 Parameters of the wind gust model and the wind turbine model. 13

2.2 Parameters of the Axial Flux PMSG model. 17

3.1 Parameters of the VSG model. 26

List of Abbrevations

P - Real Power/Active Power

Q - Reactive Power

$WECS$ - Wind Energy Conversion System

RES - Renewable Energy Resource

SG - Synchronous Generator

$PMSG$ - Permanent Magnet Synchronous Generator

$AFPMSG$ - Axial Flux Permanent Magnet Synchronous Generator

VSG - Virtual Synchronous Generator

$VISMA$ - Virtual Synchronous Machine

AC - Alternating Current

DC - Direct Current

K_p - Proportional gain

K_i - Integral gain

C_p - Power Coefficient

V - Wind Speed

T_m - Mechanical Torque

L - Inductance

C - Capacitor

SC - Super Capacitor

PLL - Phase Locked Loop

PWM - Pulse Width Modulation

Chapter 1

INTRODUCTION

Global warming is increasing by the human activity. Most of the global warming emissions are coming from the fossil fuels like coal and natural gas. To reduce these emissions renewable energy resources are being used for electricity generation. Renewable energy has the advantages that it is abundant, clean, and is economical [4]. There are many renewable energy sources, for example, geothermal, solar, wind, and tidal. Wind Energy is one of the most favorable renewable energy resources for electricity generation because of its cost compared to the other renewable energy resources and is significantly increasing year by year worldwide. As of 2016, the graph of global wind power capacity is shown in figure 1.1. The total installed wind power capacity by 2017 in United States is shown in figure 1.2

The key technologies of the wind power systems are wind turbine technology, PMSG technology, control technology and energy storage technology. There are different types of generators which are used generally for wind power applications. These include turbines with fixed and variable speed generators. Both induction and synchronous generators are used in wind energy conversion systems. There are three different types of rotors in induction generators: squirrel cage rotor, wound rotor with slip control and doubly fed induction rotors. A doubly fed induction generator is used for the wide range of speed variation. On the other hand, Permanent Magnet synchronous Generator (PMSG) is used for the low output power because of its higher efficiency and the maintenance is low because it does not have rotor current. The other advantage of

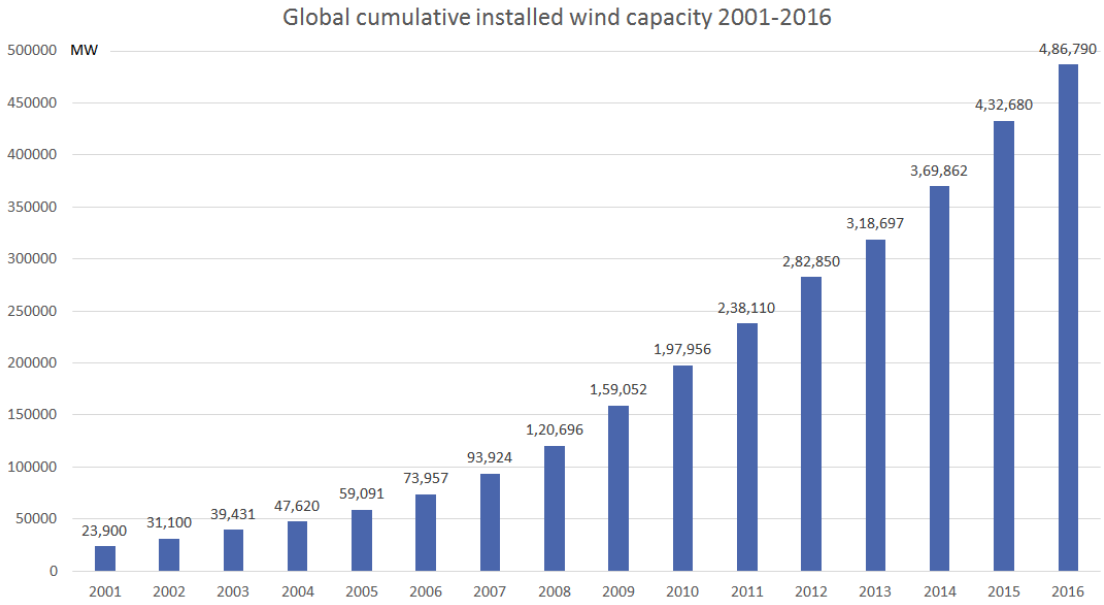

Figure 1.1: Global growth of installed wind power capacity [1]

PMSG is that it does not require a gear box which reduces the cost and weight of the nacelle [5]. PMSG is divided into Radial Flux Permanent Magnet (RFPM) and Axial Flux Permanent Magnet (AFPM) generators. When compared to RFPM, AFPM has higher power density, smaller volume, less mass and can operate at low speeds with high efficiency [6]. Based on the above advantages Axial Flux PMSG is suitable for the small wind power systems.

In conventional power systems, the bulk synchronous generators play a most important role for the power stability. The frequency regulation and the voltage control are achieved by the inertia and damping properties of the synchronous generator. Due to the lower mass of the PMSG, there is a need to replicate the inertia and damping properties virtually the same as the conventional SG.

The output power of the wind farm is fluctuating, due to the fluctuations in the wind velocity. The wind power fluctuations cause problems like frequency deviation, voltage fluctuation, low power quality and is harmful to sensitive loads. In order to improve the power stability, there is a need to provide the virtual damping and the virtual inertia. This is achieved by power electronic converter with an appropriate

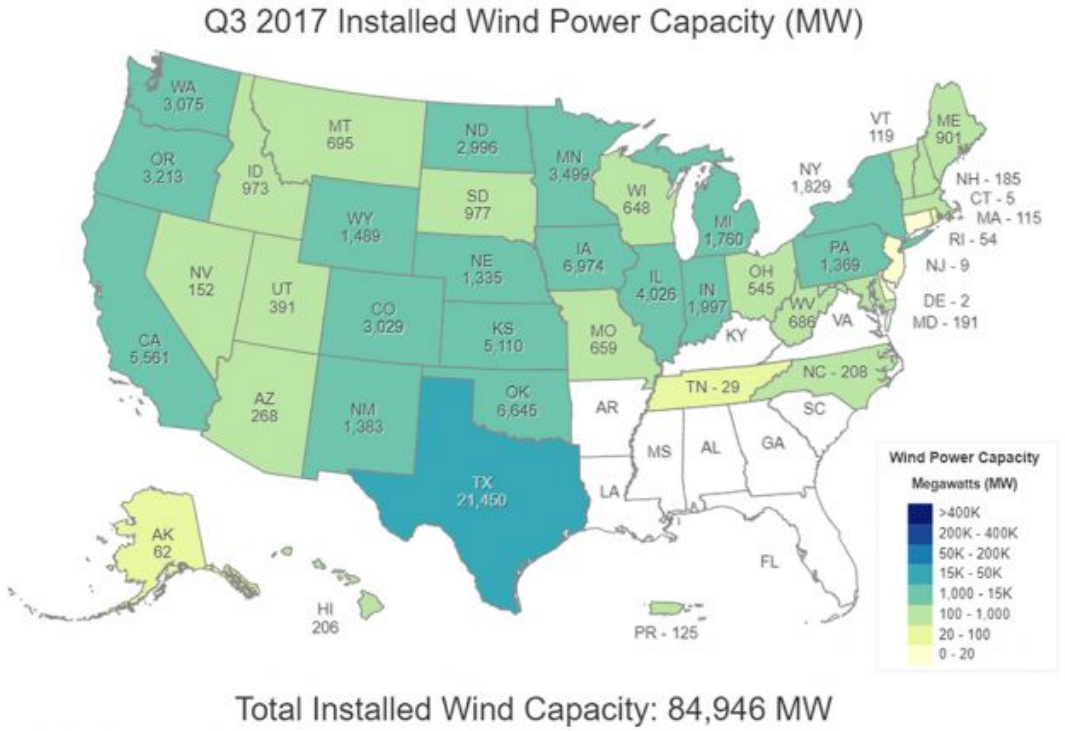

Figure 1.2: Installed wind power capacity in US by 2017 [2]

control mechanism. This is called Virtual synchronous generator (VSG).

The power control uses Energy Storage System (ESS), such as the battery, the super capacitor, etc. The storage capacity of the battery strongly dependent on age, temperature and number of cycles where as the super capacitor has advantage over a chemical battery regarding resiliency. Based on the above advantages, we have chosen a super capacitor to smooth the output power of the WTs.

A super capacitor, which is the energy storage system, is used along with the VSG coupled with the power converter with the control method. The basic structure of the VSG is shown in the below figure 1.3 [3]. The wind energy source is connected to the grid through the VSG. It acts like a synchronous generator by giving virtual inertia and damping. The VSG block regulates the output of the inverter based on the difference between the reference frequency and the measured grid frequency which is same as the

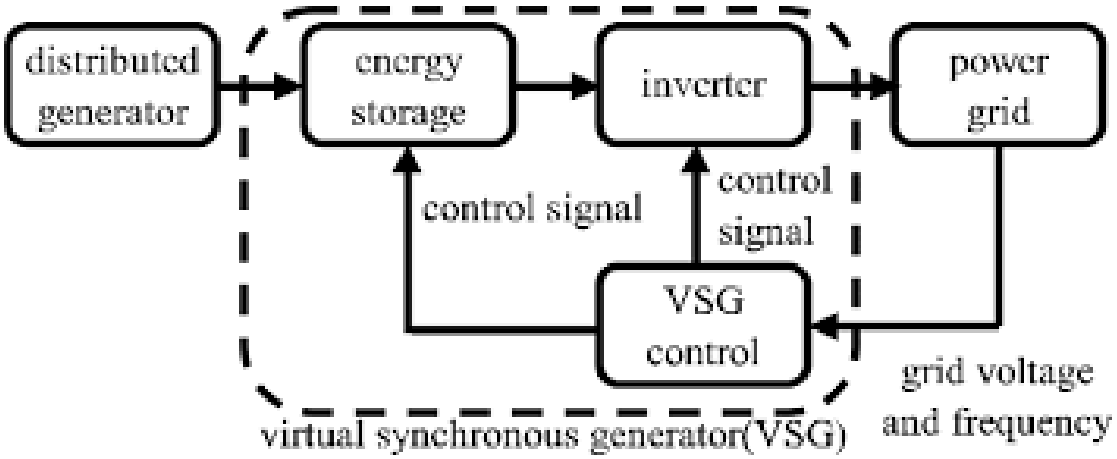

Figure 1.3: Virtual Synchronous Generator [3]

conventional system.

1.1 Literature Review

In the literature review, a survey of different topics on variable speed small wind turbine and generator system modeling which is used in the WECS will also be presented. Wind turbines generators frequently used squirrel cage induction generators previously to produce power. These generators were not able to provide stability in voltage and frequency. Because of this, the focus is changed to variable wind speed wind turbines. Later, Doubly Fed Induction Generators are used because of their advantages over the squirrel cage induction generators [7] [8]. These can provide control over the active and reactive power. power quality is also improved. These are mainly used in the large wind turbines with megawatt scale output power. In this thesis, for small wind turbine systems, Axial Flux PMSG is used because of higher efficiency and low maintenance. AFPMSG does not require gear box which reduces the weight, size and the cost [6].

Many authors have worked on the full rated power converter system used in PMSG wind conversion systems. H-bridge converters and neutral point clamped converters were designed by Xibo yuan et al for the PMSG wind power generation systems as part of prior work [9]. These converters are medium voltage and high power which are connected in series which eliminates the grid side step-up transformer. The

other type of converter which is used along with the PMSG is a Z-source inverter which works as a bridge between the generator and the grid [10]. The author in [11] designed a matrix converter which has been used along with the PMSG which eliminates the bulky storage capacitors resulting in AC-AC power conversion system. Ming Yin et al. [12] designed a model of a variable speed wind turbine system with radial flux PMSG. This generator is a high-speed generator that requires a gear box which is connected to the wind turbine. The authors in [13] and [14] also presented their model of PMSG for variable speed wind turbine systems. However, the design and modelling of the Axial Flux PMSG with coreless stator and rotor, and a super capacitor embedded in it for a wind turbine power generation system has not been presented. This thesis proposes such a system. The author in [15] used a battery for the energy storage system in the wind power generation system. But the battery has limited capacity to store the energy. In this work, the Super capacitor is used for the energy storage system which has resiliency for repeated charging and discharging.

Up to now only large wind turbines with a nacelle height of more than 60m and with output of MW have been discussed. For the small companies and industries, small sized wind turbines are going to be introduced in this thesis. Small wind turbines have a shaft of height around 12m and with output power smaller than 35 kW. However, there is a question of why the technology of large wind turbine cannot be applied to the small wind turbines. There are some differences between these in the construction and operation [13].

1. At 15m height above the ground wind is less stable than at 50m. The wind power is mostly dependent on the wind speed. This causes a lot of variation in the output power. Because of this, small wind turbines must change the speed of the shaft quickly so that the wind turbine maintains a constant output power.

2. The output power of small wind turbines is lower. Because of this, it is less complicated for power electronics (AC-DC and DC-AC Converters) to convert the full rated power and inject the power into the grid.

3. For Large wind turbines, a gear box is used to increase the rotor speed of the generator for maximum output power. For small turbines, there is no gear box which reduces the cost, weight, and the maintenance.

Because of a lack of inertia in small scale renewable energy sources RESs, there are disturbances in the output power and frequency. This could be resolved by using the VSG which provides inertia and damping properties similar to the regular synchronous machine but virtually. In a RES, there are two types of operation modes, one is the grid connected mode and the other one is the islanded mode. In this thesis, islanded mode is used to run the simulation.

The VSG concept was introduced in 2008 to maintain stable power in the renewable energy sources RESs [16], [17]. Different types of VSG topologies were introduced to replicate the inertia and damping properties of the conventional synchronous generator. The VSYNC project was conducted under the 6th European Research framework program [18] [27-32]. In this VSG topology, grid voltage is given to the PLL which produces a VSG reference current and this current reference is used to drive the power electronics converter. PLL provides a response similar to the synchronous generator. The second method of VSG comes from the Institute of Electrical Power Engineering IEPE [19], [20]. In this method, grid voltage (current) is used to generate the reference current (voltage). The amount of inertia and the damping effects are set by adjusting the virtual excitation and the virtual torque. The third method of VSG comes from Kawaski Heavy Industries (KHI) [21]. This topology is based on the algebraic type model of SG. Using the reactive power, reactive power feedback signal and the voltage feedback signal, Automatic Voltage Regulator (AVR) produces the electromotive force. Using the active power, active power feedback signal and the reference angular velocity, a governor model produces the load angle. Load angle and EMF are used to produce reference signals to drive the inverter. The fourth example comes from the ISE laboratory in Osaka University [3], [22]. The fifth type is the synchroconverter that mimic the properties of the synchronous generator [23].

This chapter of this thesis introduced the literature review of the wind energy

conversion systems and the power electronics used in this wind power system. The second chapter presents the modeling of the dynamic wind gust, wind turbine and the Axial Flux Permanent Magnet Synchronous Generator (PMSG).

The third chapter presents the modeling of the super capacitor and the bi-directional DC-DC converter with a controller to maintain the output constant.

The fourth chapter discusses the VSG topology and the control algorithm for the grid side converter.

The fifth chapter will discuss and analyze the results of the Wind energy generation system Simulink model. The sixth chapter is the conclusion and future work.

1.2 Objective

The Objectives of this thesis are itemized as following:

1. Develop a small scale wind turbine with dynamic wind gust as input.
2. Develop a viable enhanced Axial Flux Permanent Magnet Synchronous Generator (PMSG) with Virtual Synchronous Generator (VSG) characteristics.
3. Incorporate a super capacitor which is embedded in the Axial Flux PMSG to maintain the output power constant.
4. Implement a VSG model which is a power electronic converter with control mechanism.
5. Run the simulation with variable wind speed in the matlab simulink software.

1.3 Motivation

There has been interest in small wind power systems with low wind speed for

regional areas and for small businesses. Designing a viable system that can compete in the small wind market and provide a cost-effective renewable energy generation for consumers and small businesses is the main goal of the thesis. The other goal is to achieve high-power quality which means enhanced stability in the output power of the WT under conditions of variable wind speed. This is achieved by using VSG and the super capacitor to store the energy when the wind speed is greater than the nominal wind speed and deliver energy when the wind speed is lower than the nominal wind speed.

Chapter 2

MODELING AND ANALYSIS OF WIND TURBINE SYSTEMS

2.1 Introduction to Wind Turbine Systems

The main modeled components of the small-scale wind energy conversion system (WECS) are the dynamic wind gust, wind turbine and the Axial Flux PMSG. The wind turbine captures the power from the wind and the AFPMSG converts the mechanical power into electrical power. In this chapter, the mathematical models of the wind turbine and the AFPMSG will be developed and analyzed.

2.2 Wind Turbine Modeling

First we develop a model of the wind turbine. Since the wind turbine is an energy converter, the available energy stored in the wind needs to be determined. The energy in the wind is the kinetic energy of a large amount of air particles with a total mass of M, moving with a speed of V. Let us assume the wind is moving at the same speed and direction before hitting the rotor blades of the wind turbine, then the kinetic energy stored in the wind can be given by the following expression [24]:

$$E = \frac{1}{2}MV^2 \tag{2.1}$$

where E is the kinetic energy of the air particles, m is the mass of the air particles and V is the wind speed. The total mass of the air particles m, for a period of time t is given

by the equation:

$$M = \rho AVt = \rho\pi r^2 Vt \tag{2.2}$$

where ρ is the density of the air, A is the area swept by the blades of the wind turbine and r is the radius of the rotor. By substituting (2.2) in (2.1) , the kinetic energy of the air particles is given by the following equation [25].

$$E = \frac{1}{2}\rho\pi r^2 V^3 t \tag{2.3}$$

The aerodynamic wind power at time t [26] is given by

$$P_{wind} = \frac{E}{t} = \frac{1}{2}\rho\pi r^2 V^3 \tag{2.4}$$

Where P is the power of the wind. From the above equation (2.4), power is directly proportional to the cube of the wind velocity and is directly proportional to the radius of the wind turbine rotor.

The power in the above equation (2.4) is the total power of the wind. But the portion of this power can be captured by the wind turbine. In [27] Albert Bertz presented the idea that after hitting the wind turbine rotor blades, the wind velocity decreases. It means some kinetic energy is left in the wind after hitting the rotor blades.

The power coefficient of the wind turbine is the ratio of the power captured by the wind turbine to the maximum power in the wind.

$$C_P = \frac{P_{Turbine}}{P_{Wind}} \tag{2.5}$$

The power coefficient of the wind turbine can be expressed by [28] :

$$C_P = c_1(c_2\frac{1}{\alpha} - c_3\beta - c_4\beta^x - c_5)e^{-c_6\frac{1}{\alpha}} \tag{2.6}$$

where the values of the coefficients $(c_1, c_2, c_3, c_4, c_5, c_6)$ depends on the type of the wind

turbine. In this $c_1 = 0.5176, c_2 = 116, c_3 = 0.4, c_4 = 5, c_5 = 21, c_6 = 0.0068$ [29] and

$$\frac{1}{\alpha} = \frac{1}{\lambda + 0.08\beta} - \frac{0.035}{1 + \beta^3} \tag{2.7}$$

where β is the pitch angle of the blade space. The pitch angle is the angle between the orientation of the blade and the wind velocity. When the pitch angle is zero, the blade is fully impacted by the wind velocity, and the wind turbine will capture the maximum power in the wind. λ is the tip speed ratio which is defined as the ratio between the rotor speed and the wind speed. The tip speed ratio is given by the equation [29]:

$$\lambda = \omega_m r / V \tag{2.8}$$

where ω_m is the angular speed of the wind turbine generator and r is the rotor radius.

The wind turbine is used to convert the wind kinetic energy to mechanical energy. Wind passes over the blades, starts rotating the blades and exerting a turning force. The rotating blades of the wind turbine turns a shaft inside the nacelle that goes into the gear box.

The gear box is used to increase the rotational speed which is appropriate for the generator. In small turbines the gear box ratio is 1:1, that is the angular speed of the wind turbine rotor is equal to the rotor speed of the generator. The mechanical torque T_m is defined by [30]

$$T_m = \frac{P_m}{\omega_m} = \frac{1}{2\omega_m} \rho \pi r^2 V^3 C_p(\lambda, \beta) \tag{2.9}$$

The simulink model of the wind turbine is modeled by using the above equations (2.6, 2.7, 2.8, 2.9) which is shown in figure 2.1. The parameters of the wind turbine model is shown in the table 2.1.

A wind gust is a sudden increase of the wind speed which does not lasts more than 15 sec. This is modeled by multiplying a constant wind speed with the random fluctuations derived from the white noise block in MATLAB/SIMULINK The simulink

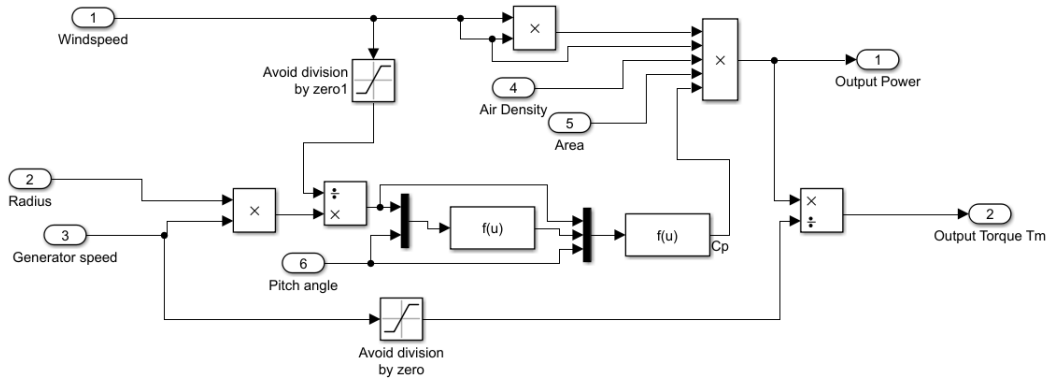

Figure 2.1: Simulink model of the wind turbine

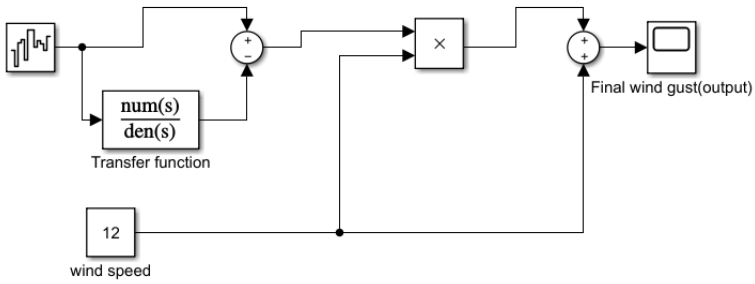

Figure 2.2: Simulink model of the wind gust

model of the dynamic wind gust is shown in figure 2.2.

The figure 2.3 shows the wind speed with mean value of the wind speed is 12 m/s and fluctuations around mean value.

Table 2.1: Parameters of the wind gust model and the wind turbine model.

Parameter	**Value**
wind speed	12 m/s
Radius of the rotor blade	5 m
Air density	1.225 kg/m^3
pitch angle	0
Area	77 m^2

2.3 Modeling of Axial Flux Permanent Magnet Synchronous Generator

2.3.1 Introduction to PMSG

Synchronous machines are frequently used in wind turbine applications for their ability to generate variable power factor energy. There are two types of synchronous machines, brush and brushless. For the machines with brushes, the excitation is done using brushes and slip rings on the shaft and this requires high maintenance. The other one is the brushless machine which uses permanent magnets for the excitation instead of electromagnets. The other advantages are it does not require a separate external DC source for field winding because the permanent magnets create a constant magnetic field. In the permanent magnet synchronous generator, the permanent magnets are used for the excitation. In this thesis, two rotors with the permanent magnets mounted on it and one core-less stator are used yielding axially oriented flux lines. The synchronous generator characteristics are implemented in an axial flux design by providing modeled electronic power conversion which ensures power is generated with configurable power factor. PMSG is used in low power and low-cost synchronous generator.

Axial Flux core less PMSG is the suitable generator for small wind turbines because of less complexity in design and manufacture. The core less design of the machine eliminates the cogging torque which means the torque produced by the interaction between the magnets on the stationary rotor and the rotating stator. It also reduces the weight and increases the efficiency when compared to the conventional design.

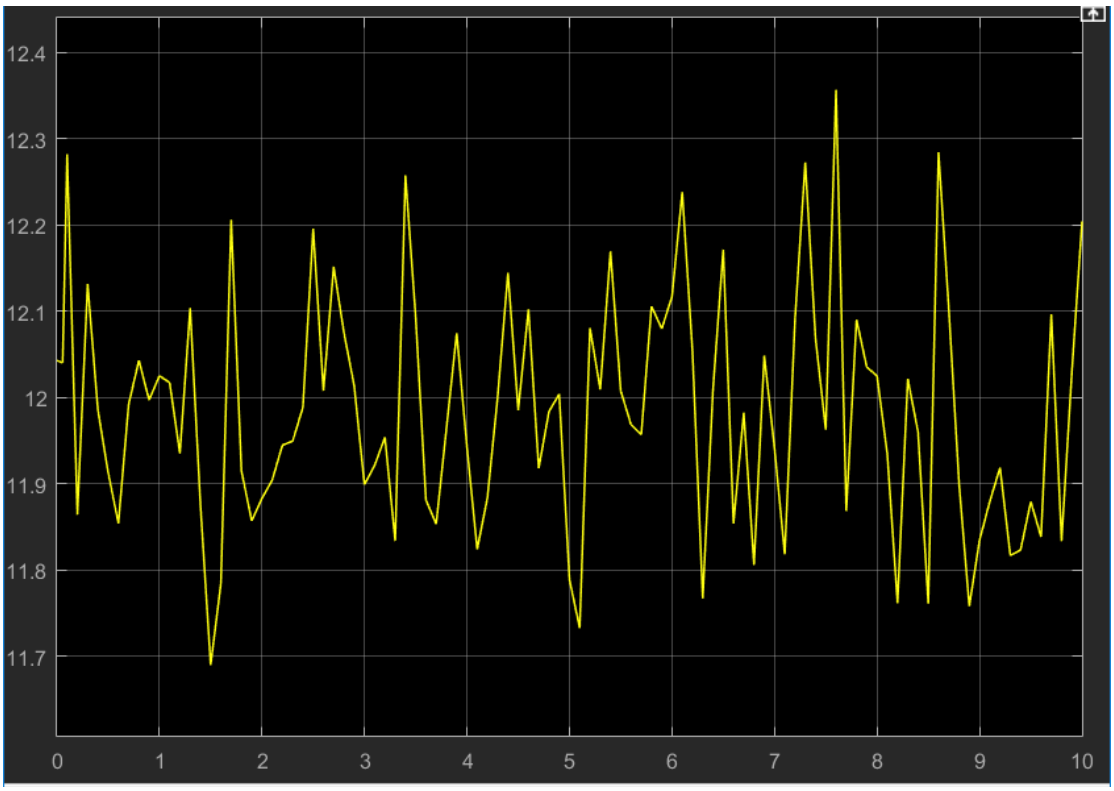

Figure 2.3: Dynamic wind gust.

2.3.2 Mathematical Model of the AFPMSG

AFPM synchronous generator consists of one stator and two rotors. A coreless stator is used to eliminate the stator iron losses and rotor with permanent magnets. The dynamic model of the AFPM Generator is derived from the two phase synchronous frames, d-axis and q-axis. Three phases abc are converted into two phase synchronous reference frames by using Park's transformation. The dq0's transformation is a mathematical transformation which is used for the analysis of synchronous models. It was introduced by R.H. Park [31]. The abc to dq0 transformation is given by following matrix:

$$\begin{bmatrix} u_d \\ u_q \\ u_0 \end{bmatrix} = \sqrt{\frac{2}{3}} \begin{bmatrix} \cos(\theta) & \cos(\theta - \frac{2\pi}{3}) & cos(\theta + \frac{2\pi}{3}) \\ -\sin(\theta) & -\sin(\theta - \frac{2\pi}{3}) & -\sin(\theta + \frac{2\pi}{3}) \\ \frac{\sqrt{2}}{2} & \frac{\sqrt{2}}{2} & \frac{\sqrt{2}}{2} \end{bmatrix} \cdot \begin{bmatrix} u_a \\ u_b \\ u_c \end{bmatrix} \tag{2.10}$$

The inverse Park's transformation is given by:

$$\begin{bmatrix} u_a \\ u_b \\ u_c \end{bmatrix} = \sqrt{\frac{2}{3}} \begin{bmatrix} \cos(\theta) & -\sin(\theta) & \frac{\sqrt{2}}{2} \\ \cos(\theta - \frac{2\pi}{3}) & -\sin(\theta - \frac{2\pi}{3}) & \frac{\sqrt{2}}{2} \\ cos(\theta + \frac{2\pi}{3}) & -\sin(\theta + \frac{2\pi}{3}) & \frac{\sqrt{2}}{2} \end{bmatrix} . \begin{bmatrix} u_d \\ u_q \\ u_0 \end{bmatrix} \tag{2.11}$$

where u_a, u_b and u_c are the stator voltages in three phase space. The parameters u_d, u_q and u_0 represent the stator voltages in dq of the AC generator and θ is the angle between the rotor d- axis and the stator axis. The synchronization between the abc phases and the dq reference frame is maintained by using a phase locked loop (PLL) [32]. The following figure 2.4 shows the dq reference frame. The mathematical model of the

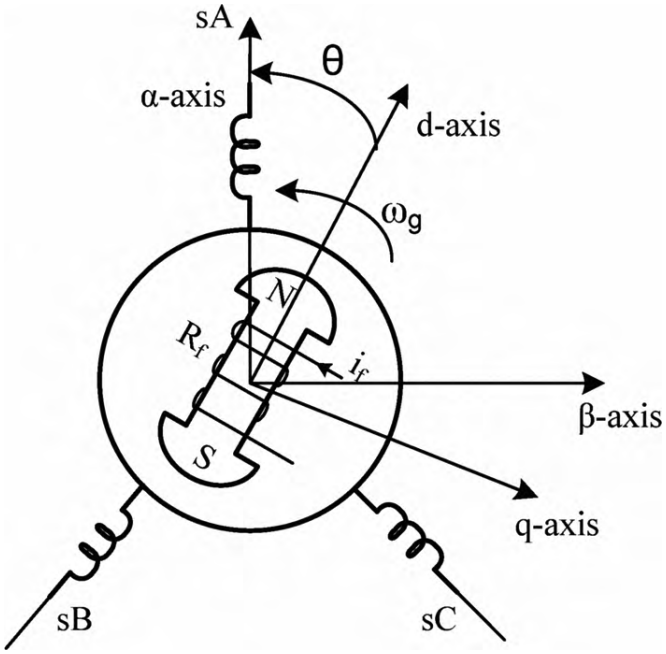

Figure 2.4: dq model of the synchronous machine

AFPM synchronous generator in the dq reference frame is given by[2]

$$v_d = R_s i_d + L_d \frac{di_d}{dt} - \omega_e L_q i_q \tag{2.12}$$

$$v_q = R_s i_q + L_q \frac{di_q}{dt} + \omega_e L_d i_d + \omega_e \varphi_f \tag{2.13}$$

Where L_d and L_q are inductances of d and q axis respectively, R is the stator resistance and φ_f is the permanent magnetic flux in weber. The parameter w_e is the electrical

rotating speed of the generator in radians per second. The equivalent circuit of the AFPM synchronous generator is shown in the figure 2.5. The electric power expressed

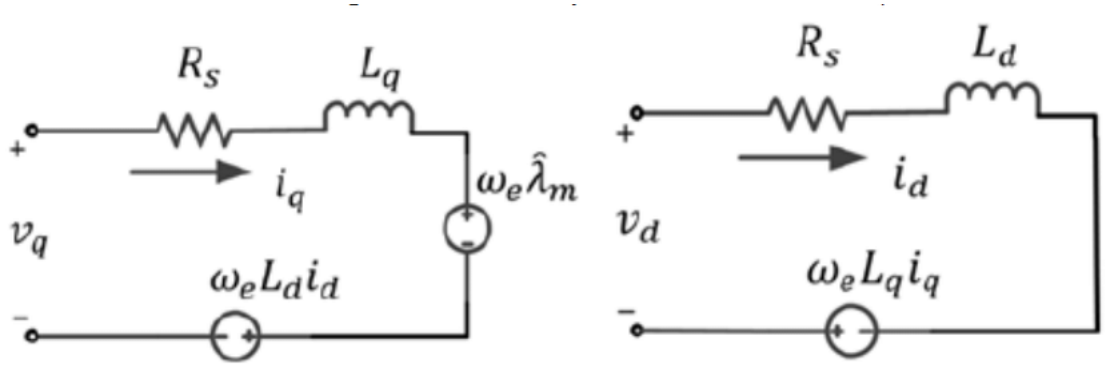

Figure 2.5: Equivalent circuit of AFPMSG q-axis and d-axis respectively.

in the three phase abc reference frame is given by:

$$P_{abc} = v_a i_a + v_b i_b + v_c i_c \tag{2.14}$$

The power in dq-reference frame is given by:

$$P_{dq} = \frac{3}{2}(v_d i_d + v_q i_q) \tag{2.15}$$

The electromagnet torque is given by the equation [30]:

$$T_e = 1.5P((L_d - L_q) i_d i_q + i_q \varphi_f) \tag{2.16}$$

where p is the number of pole pairs of the generator.

The simulink model of the AFPMSG is modeled by using the above equations 2.12, 2.13 and 2.14 and it is shown in the figure 2.6. The parameters of the AFPMSG is shown in the table 2.2.

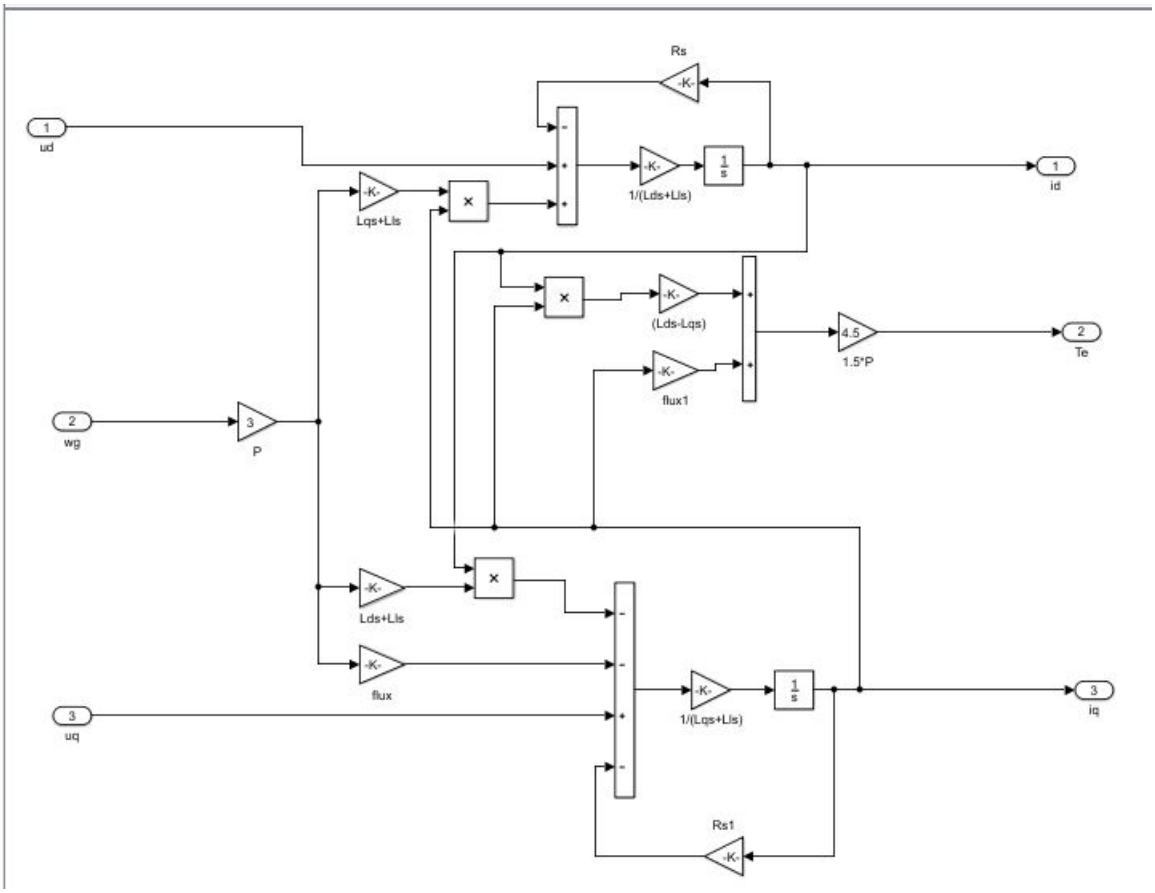

Figure 2.6: Simulink model of the AFPMSG.

Table 2.2: Parameters of the Axial Flux PMSG model.

Parameter	**Value**
Number of pole pairs	8
Stator resistance	0.821 m Ω
Inductance	1.53 mH

Chapter 3

MODELING OF VIRTUAL SYNCHRONOUS GENERATOR

3.1 Introduction

In the chapter 1 literature review, various topologies and control methods of VSG were discussed. The basic operation of VSG provides real power and reactive power. In this chapter the implementation of the VSG structure with mathematical model will be introduced. In this thesis an islanded micro grid is considered, which is highly recommended for small business and factories. The brief overview of the VSG with Islanded mode is shown in figure 3.1. The primary source of energy is the DC voltage which is coming from the RES (Wind Power system) and super capacitor storage. The Distributed Generation (DG) source is connected to the inverter that converts DC to AC at 60 Hz frequency. The inverter output is connected to the LC filter to eliminate the harmonic distortion. The load is connected to the inverter via LC filter. The VSG controller is used to produce gate signals to control the inverter for the desired power supply to the grid.

The three phase voltage and the current from the load bus are used to measure the active power and the reactive power. Three phase measurements are converted into dq using Park's transformation. To maintain the voltage and the frequency stable, droop controllers are used [33]. A P-F droop controller is used to compute frequency of the VSG which is used to calculate the phase angle. A Q-V droop controller is used to

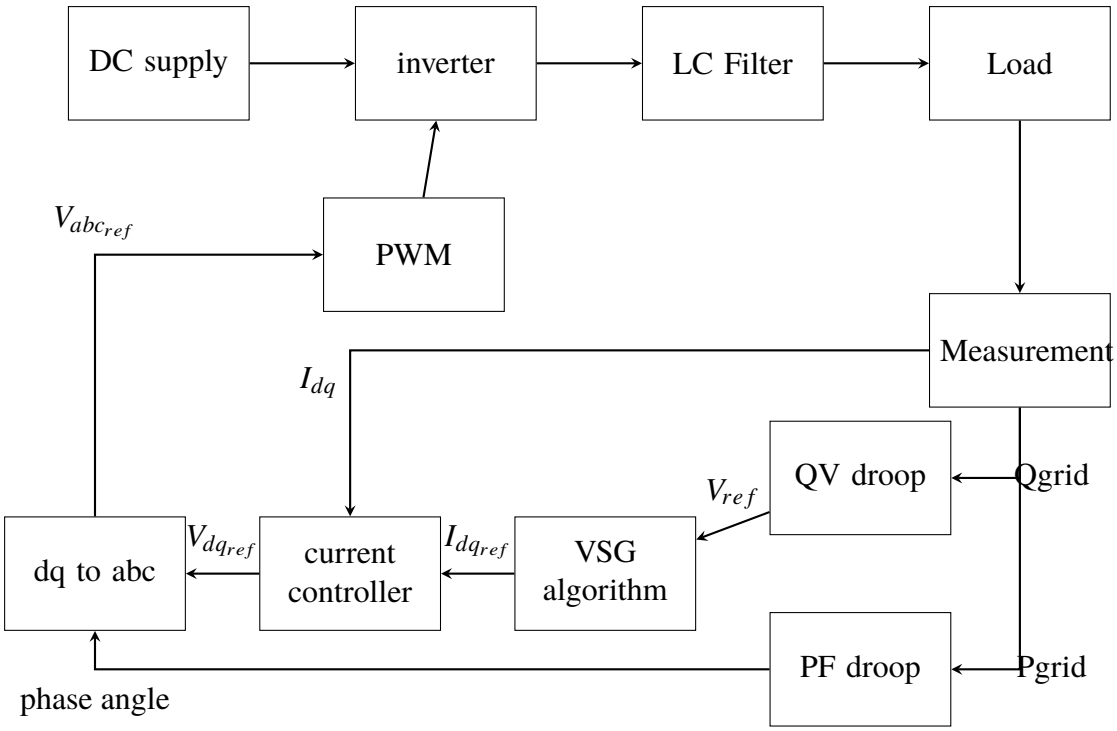

Figure 3.1: Brief Overview of VSG topology

compute the reference voltage. The synchronous algorithm uses the reference voltage to produce the reference current which is given to the current controller. The current controller computes three phase reference voltage. By using the three-phase reference voltage and the phase angle produced by the P-F droop controller, the PWM provides gate pulses to the inverter to yield the desired real and reactive power.

3.2 Real Power - Frequency Droop Control

To stabilize the output power of the generator, frequency control should have a drooping characteristic with respect to the generator output. The power- frequency droop characteristic is shown in below graph (figure 3.2) and is expressed by the following equation [34].

$$F_{load} - F_{nom} = -s(P_{load} - P_{nom}) \tag{3.1}$$

$$F_{load} = F_{nom} + s(P_{nom} - P_{load}) \tag{3.2}$$

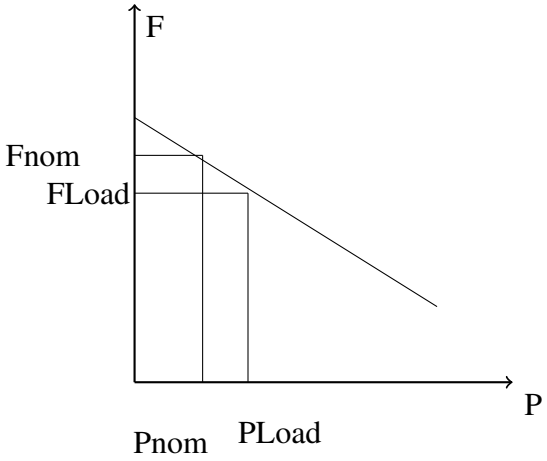

Figure 3.2: PF droop characteristics.

where F_{load} is the reference grid frequency, F_{nom} is the nominal frequency, s is the $P-F$ droop coefficient, P_{load} is the measured three phase grid active power and P_{nom} is the nominal real power. By using equation 3.2, $P-F$ droop control model is implemented in simulink and is shown in figure 3.3.

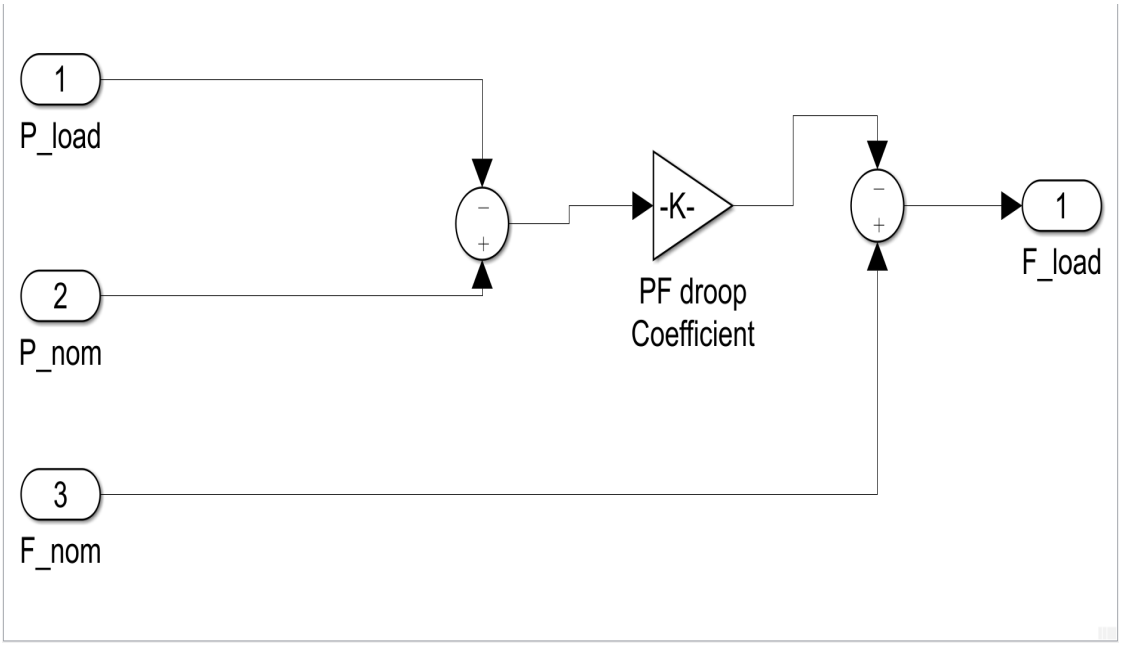

Figure 3.3: Simulink model of the PF droop control.

If there is any change in the load demand, the frequency will drop (increase) which causes the prime mover to increase (decrease) the supply and hence increase

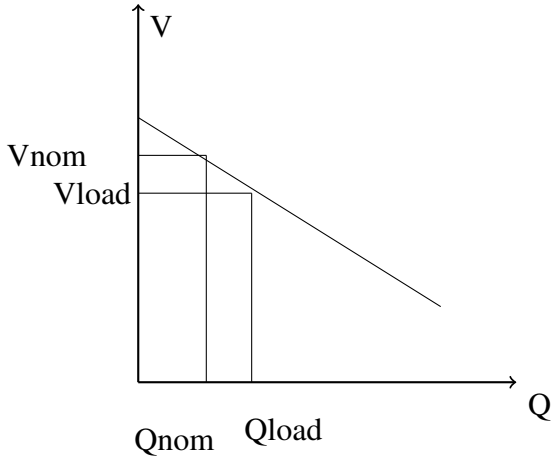

Figure 3.4: QV droop characteristics.

(decrease) the frequency. This is achieved by using the $P - F$ droop controller. In this thesis nominal frequency is 60 Hz.

3.3 Reactive Power- Voltage Control

The grid/ load voltage is related to the reactive power of the generator. The Q-V droop characteristics are shown in the below figure 3.4. The Q-V droop characteristic is given by the following equation [34]

$$V_{load} - V_{nom} = -n(Q_{load} - Q_{nom}) \tag{3.3}$$

$$V_{load} = V_{nom} + n(Q_{nom} - Q_{load}) \tag{3.4}$$

Where V_{load} is the grid voltage, V_{nom} is the nominal voltage, n is the $Q - V$ droop coefficient, Q_{load} is the measured reactive power and Q_{nom} is the nominal reactive power. $Q - V$ droop coefficient is used to maintain the voltage constant when grid voltage varies with respect to nominal voltage. By using equation 3.4, Simulink model of the Q-V droop control is implemented and is shown in the following figure 3.5.

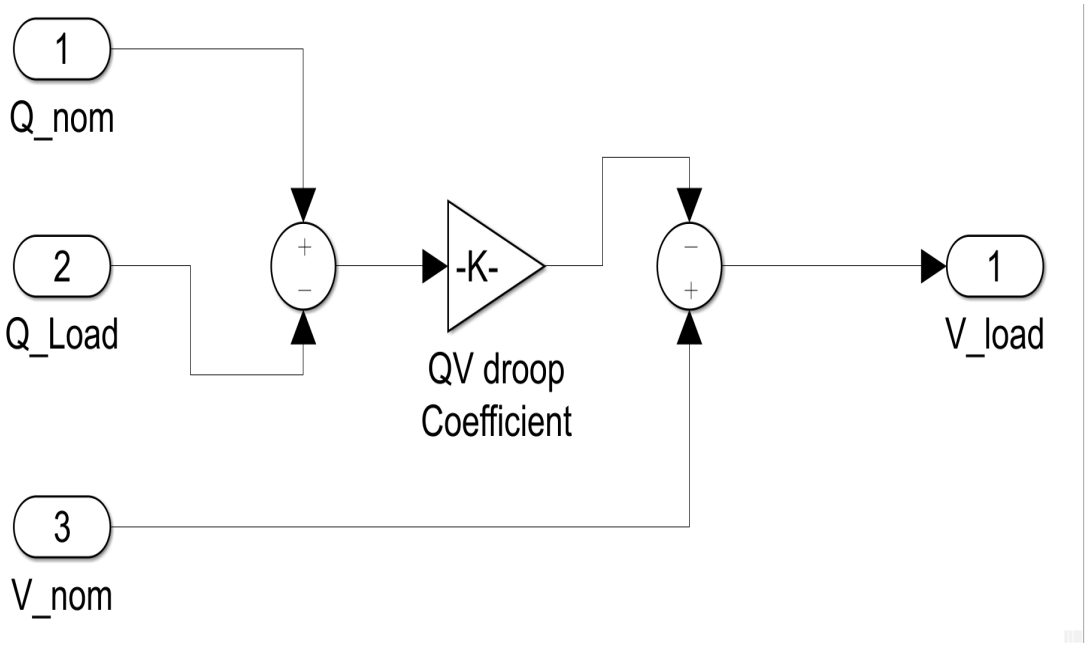

Figure 3.5: Simulink model of the QV droop control.

3.4 VSG Algorithm

The VSG algorithm is based on the synchronous generator model. It is used to produce the reference dq currents to the current control. First consider the armature resistance r_a and x_s is the generator synchronous reactance same for both the d-axis and q-axis. The equivalent circuit of the Virtual generator is shown in the following figure 3.6.

The voltage produced by the Q-V droop controller is considered as the virtual generator excitation voltage V_e. The phasor diagram of the virtual generator is shown in figure 3.7. In this q-axis I_d directed along the generator phase voltage and d-axis lead the q-axis by 90 degrees. The armature current which is reference to the current controller is calculated by using the following equation [35].

$$I_{ref} Z = V_e - V_{grid} \tag{3.5}$$

where Z is the total impedance of the virtual generator. The above equation 3.5 in the

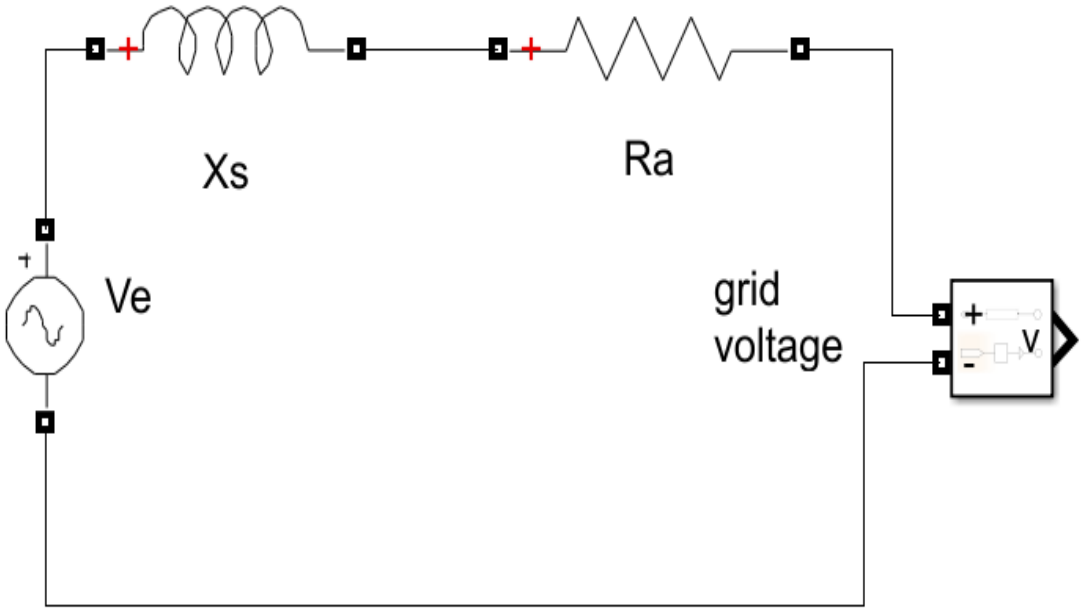

Figure 3.6: Equivalent circuit of virtual synchronous generator.

dq components is shown in the following equation [35].

$$\begin{bmatrix} I_{ref_d} \\ I_{ref_q} \end{bmatrix} = \frac{1}{Z}\left(\begin{bmatrix} V_{e_d} \\ V_{e_q} \end{bmatrix} - \begin{bmatrix} V_{grid_d} \\ V_{grid_q} \end{bmatrix}\right) \tag{3.6}$$

$$\frac{1}{Z} = \begin{bmatrix} \frac{r_a}{r_a^2+x_s^2} & \frac{x_s}{r_a^2+x_s^2} \\ -\frac{r_a}{r_a^2+x_s^2} & \frac{x_s}{r_a^2+x_s^2} \end{bmatrix} \tag{3.7}$$

By substituting equation 3.7 in equation 3.6, get the dq reference currents.

$$I_{ref_d} = (V_{e_d} - V_{grid_d})\frac{r_a}{r_a^2 + x_s^2} + (V_{e_q} - V_{grid_q})\frac{x_s}{r_a^2 + x_s^2} \tag{3.8}$$

$$I_{ref_q} = (V_{e_q} - V_{grid_q})\frac{r_a}{r_a^2 + x_s^2} - (V_{e_d} - V_{grid_d})\frac{x_s}{r_a^2 + x_s^2} \tag{3.9}$$

By using the above equations 3.8 and 3.9, the VSG algorithm model is implemented in simulink and is shown in following figure 3.8.

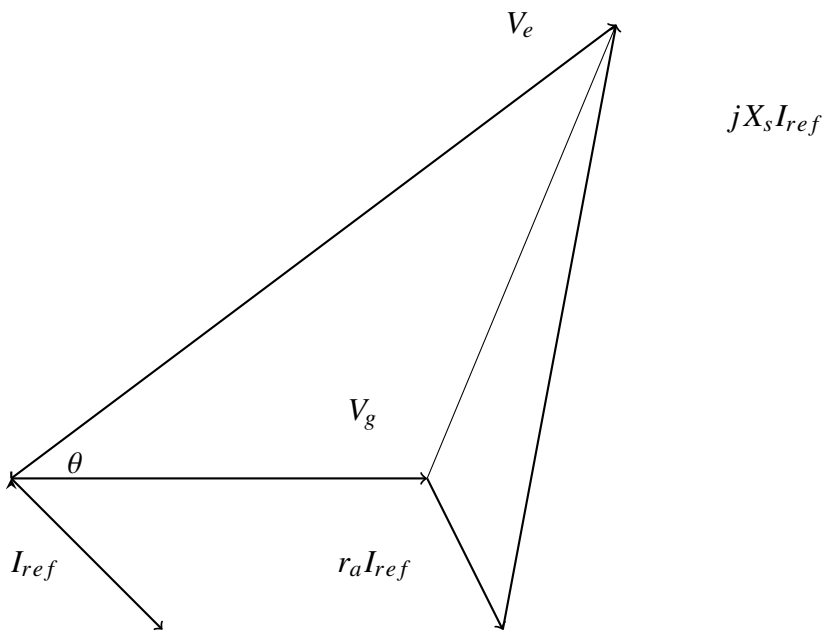

Figure 3.7: Virtual Generator phasor diagram.

3.5 Current Control

There are two types of control methods, one is current control and the other is voltage control. When compared to voltage control, current control response is very fast and sensitive. In this thesis, current control is used. LC filter is used to eliminate harmonic distortions and also to implement the current control loop. The equivalent circuit of the LC filter is shown in the following figure 3.9 [35]. Apply kirchoff's voltage law to the LC circuit in figure 3.9.

$$LI_{inv} = V_{inv} - V_{grid} \tag{3.10}$$

where L is the filter inductance, I_{inv} is the inverter current, V_{inv} is the inverter voltage and v_grid is the measured gird/load voltage. The above equation in dq components is expressed in the following equation 3.11 by using Park's transformation [36].

$$LI_{ref_d} = V_{inv_d} - V_{grid_d} + \omega_g LI_q \tag{3.11}$$

$$LI_{ref_q} = V_{inv_q} - V_{grid_q} - \omega_g LI_d \tag{3.12}$$

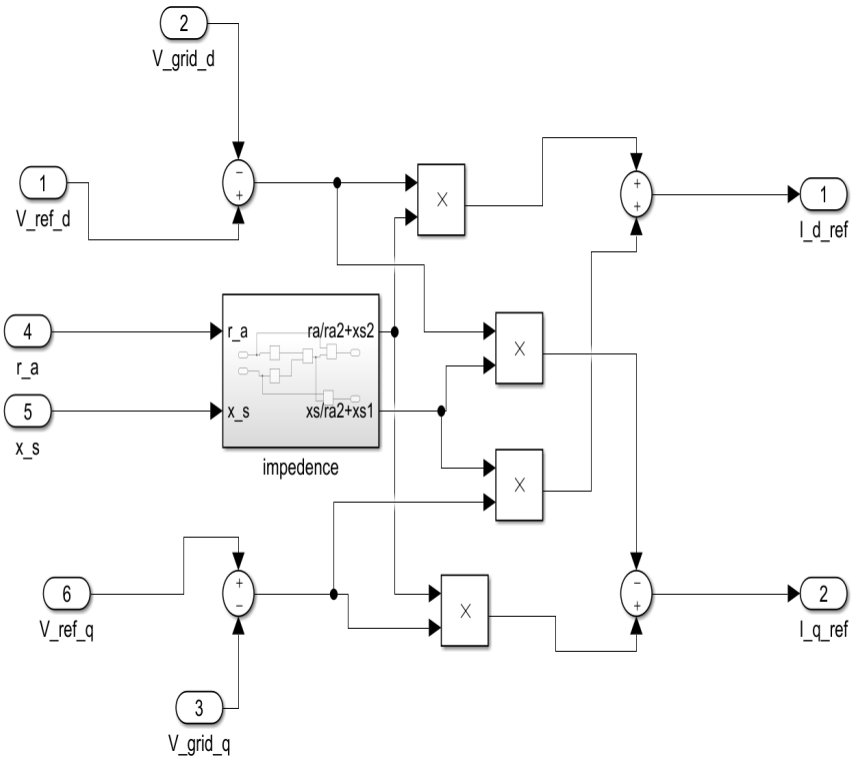

Figure 3.8: Simulink model of the VSG Algorithm.

The current controller keep track of the change in the reference current and the measured current by using proportional gain K_p and the integral gain K_i [36].

$$V_{inv_d} = V_{grid_d} + \omega_g L I_q + K_p(I_{ref_d} - I_d) + K_i \int (I_{ref_d} - I_d) \tag{3.13}$$

$$V_{inv_q} = V_{grid_q} - \omega_g L I_d + K_p(I_{ref_q} - I_q) + K_i \int (I_{ref_q} - I_q) \tag{3.14}$$

By using above two equations 3.13 and 3.14 the simulink model of the current controller is implemented and is shown in the following figure 3.10. The output dq voltages are converted into three phase reference voltages by using Park's transformation. This three phase reference voltage is used to drive the PWM generator, which controls the inverter by providing gate pulses.

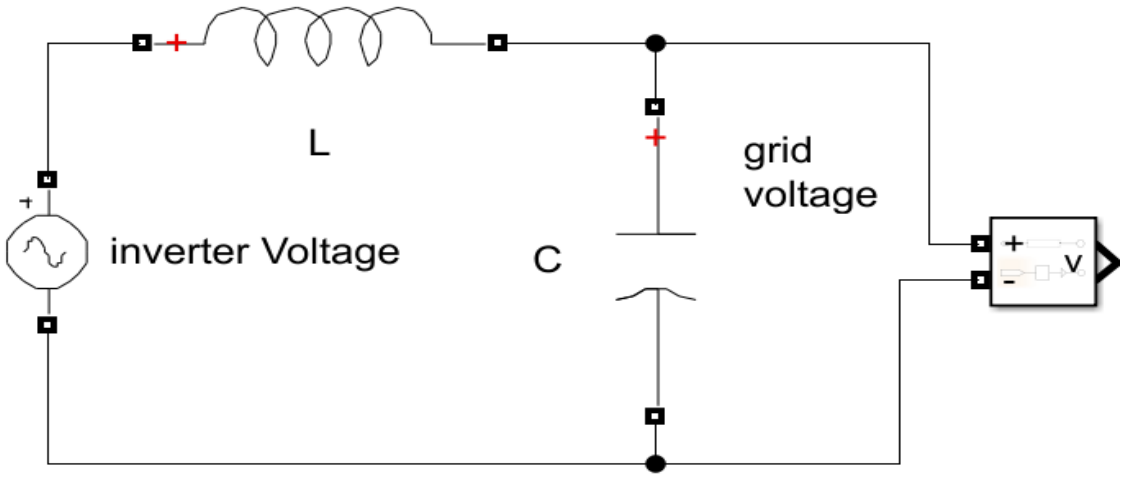

Figure 3.9: Equivalent circuit of the LC filter.

Table 3.1: Parameters of the VSG model.

Parameter	**Value**
Filter Inductance	4mH
Filter Capacitor	10μF
PF droop coefficient	0.003
QV droop coefficient	0.6
Proportional gain	0.9
Integral Gain	1.2
Nominal Frequency	60Hz

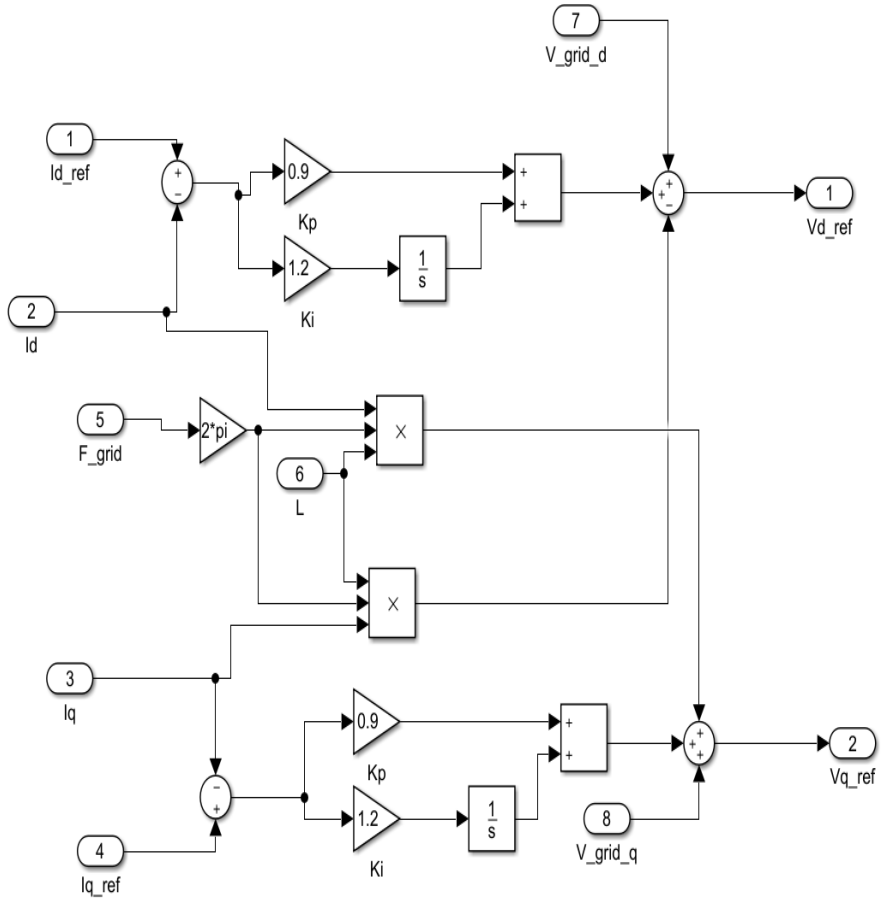

Figure 3.10: Simulink model of the Current Controller.

Chapter 4

MODELING OF THE SUPER CAPACITOR

The main cause of the output power fluctuations is the change in the wind speed. In chapter 2 the wind speed is generated by using noise and the constant speed which gives the dynamic wind gust. The super capacitor is connected to the DC link of the grid side converter. The control signals for the super capacitor are given by the control system. By using these control signals the super capacitor stores the energy (i.e. charges the capacitor) when the output real power is greater than the nominal and discharges when the output real power is less than the nominal. The control for the super capacitor is shown in figure 4.1 and 4.2.

Here IGBT diodes are used to flow the current to and from the capacitor. When the power coming from the wind turbine is lower than the nominal output power, the super capacitor discharges by delivering the sufficient power to stable the output power at nominal. And when the power coming from the wind turbine is greater than the nominal, the super capacitor charges by maintaining the constant output power. The model of the super capacitor with control is shown in the figure 4.3.

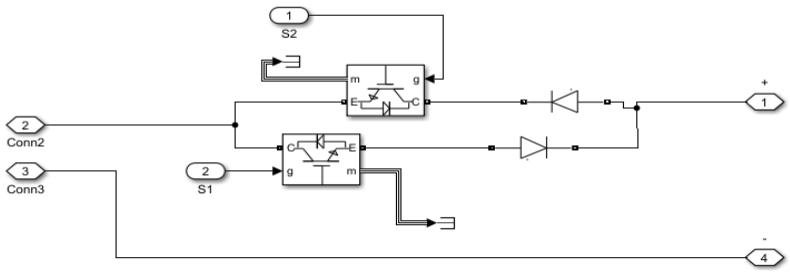

Figure 4.1: Simulink model of Super capacitor control system.

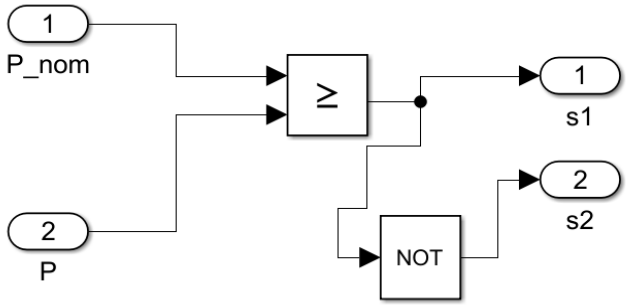

Figure 4.2: Simulink model of control signals.

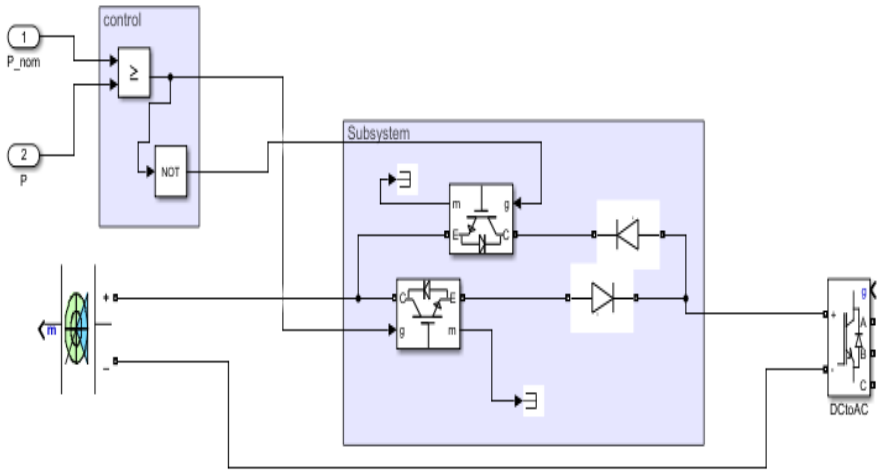

Figure 4.3: Simulink model of super capacitor with control signals connected to inverter.

Chapter 5

SIMULATION RESULTS AND ANALYSIS

In this chapter, the simulation results of the test are presented. The Dynamic simulink models are implemented in matlab simulink. The parameters of the wind turbine and the AFPMSG are presented in chapter 2 and the parameters for the VSG are presented in chapter 3. The y-axis represents time (in seconds) in all graphs in this chapter.

The first experiment is the WECS without VSG and variable wind speed. This gives the results of the uncontrolled inverter with changes in wind speed, load or other disturbances supplying power to the islanded load. The power source is the Wind energy and PWM technique is used to control the inverter. The AC frequency is taken as 60Hz and the switching frequency is 1600 Hz. The following figure 5.1 is the model of the WECS without VSG.

Figure 5.2 shows the step wind speed which is taken for the simulation of the wind power system with and without VSG control. We know that the torque is inversely proportional to the angular speed. From the figures 5.3 and 5.5 it is shown that when the wind speed has a step increase, there is a increase in the rotor speed and decrease in the torque.

At time t= 5sec the wind speed is increased from 10m/s to 12m/s. From figure 5.6 and 5.7 the voltage and current changes when there is a disturbance or change in the input. The clear sine waves of three phase voltage and current are shown in the figures 5.8 and 5.9 respectively.

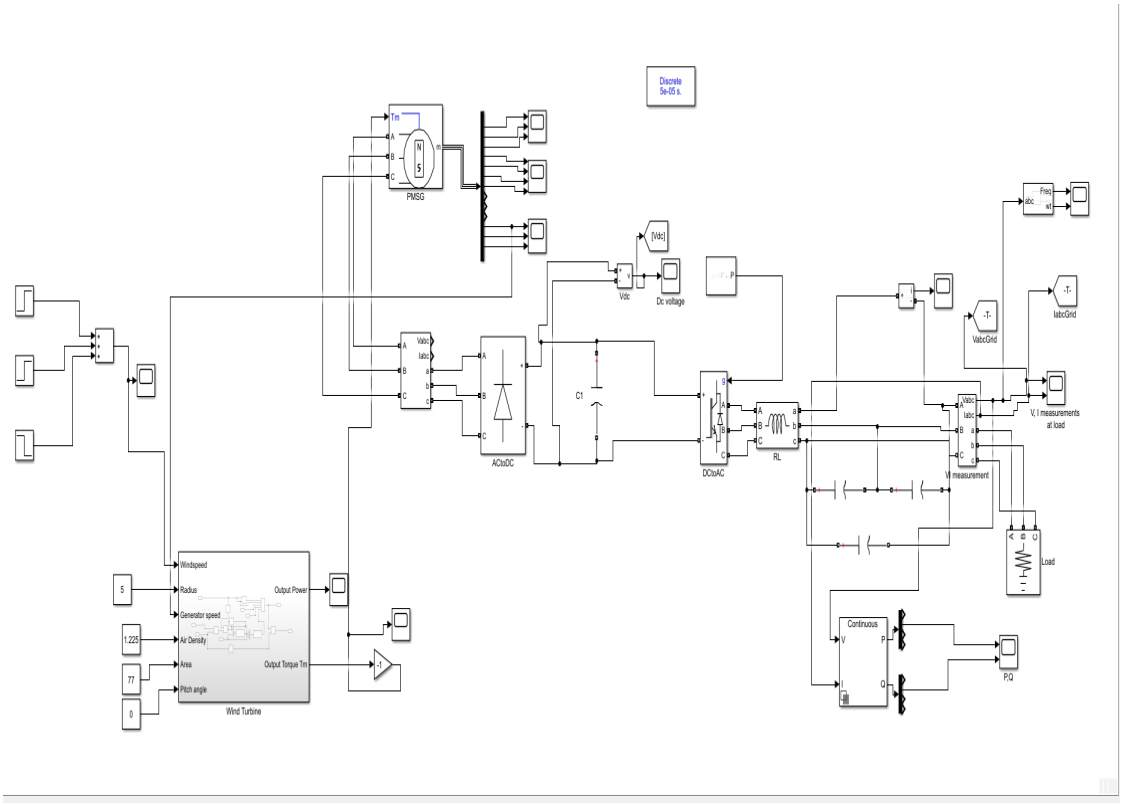

Figure 5.1: Overview of the Wind power system without control method.

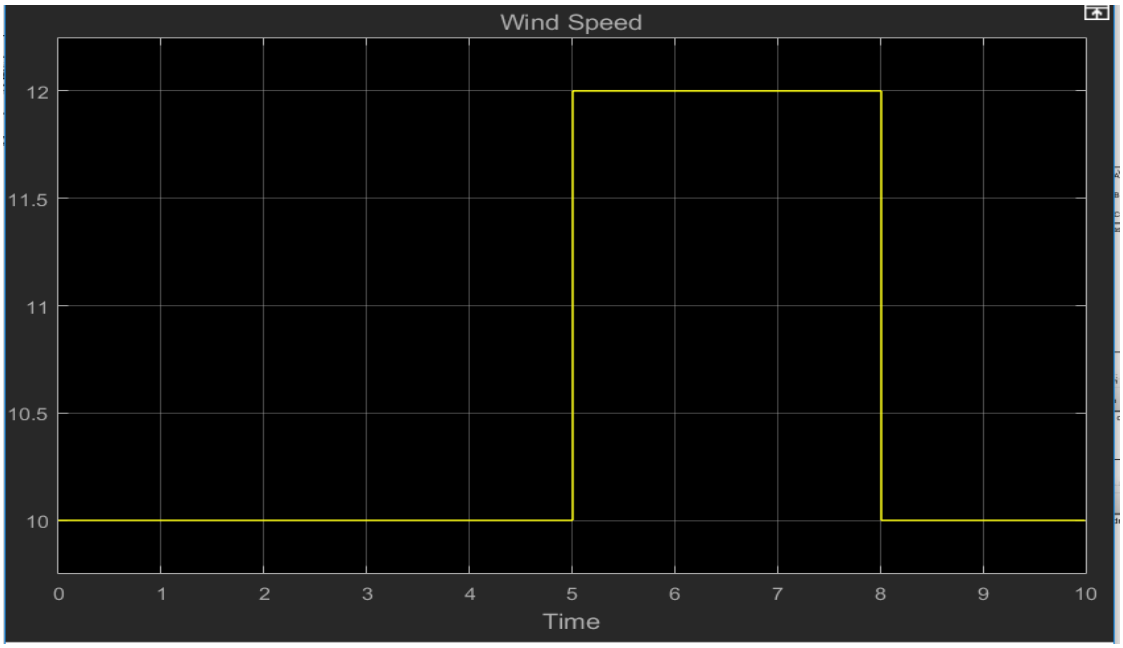

Figure 5.2: Step wind speed as input (m/s).

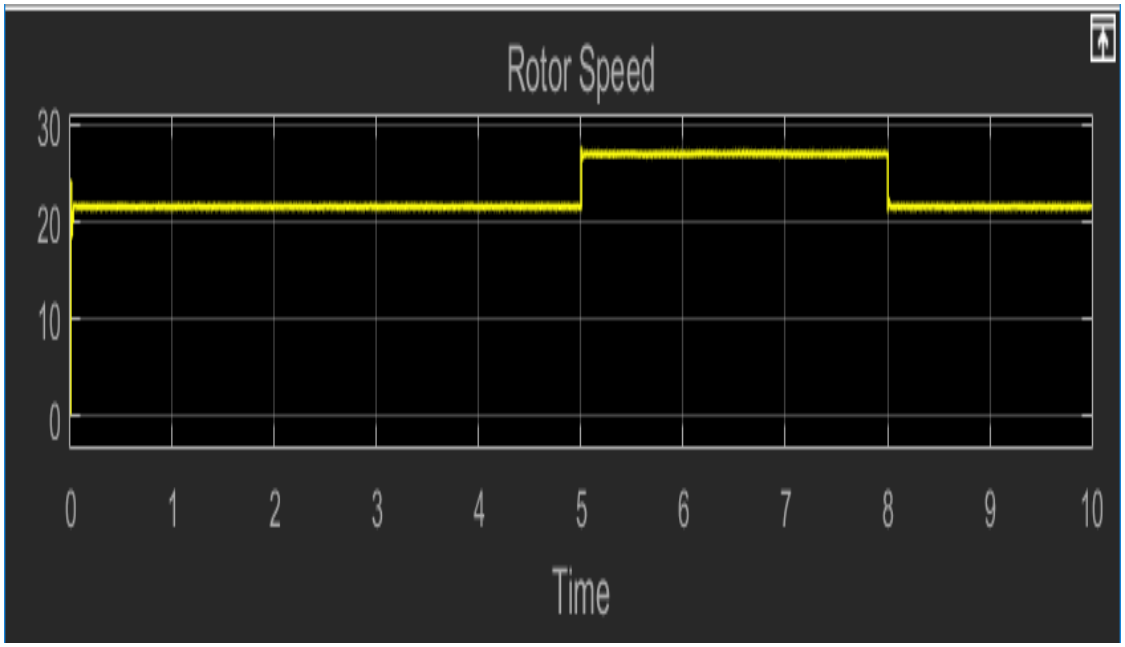

Figure 5.3: Speed of the rotor (rad/s).

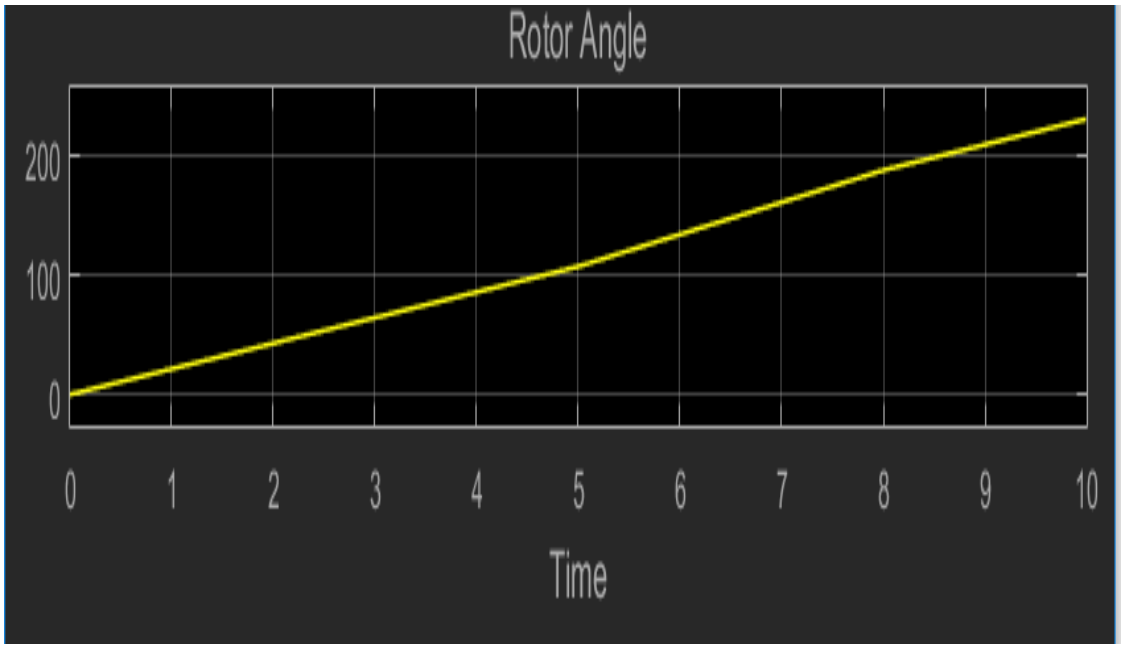

Figure 5.4: Rotor angle (rad).

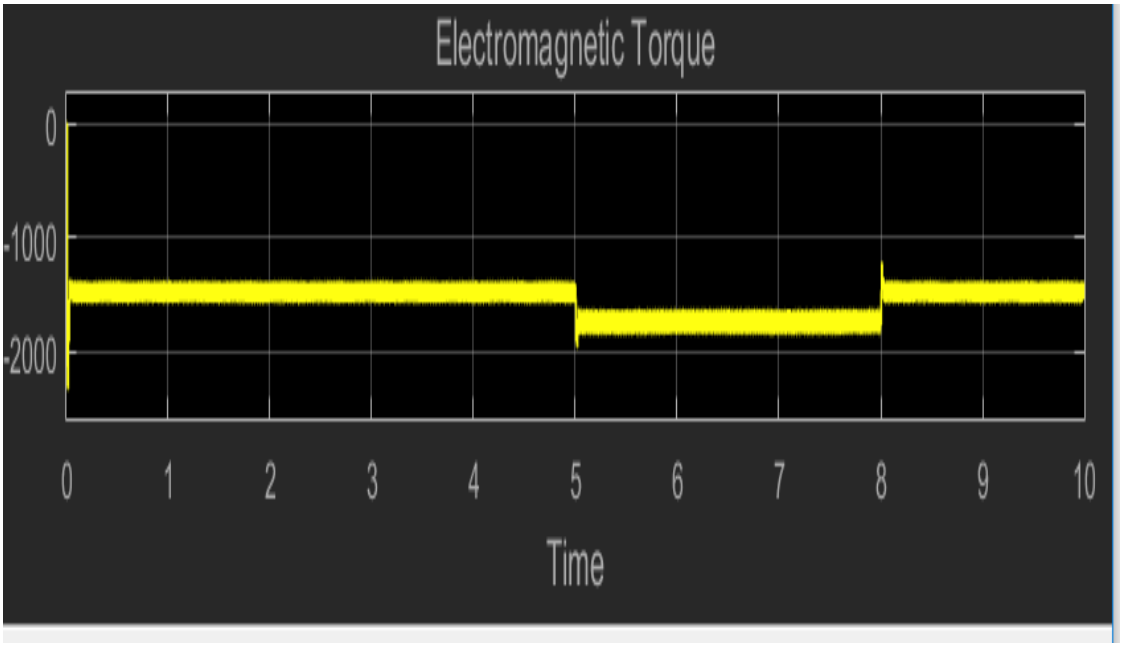

Figure 5.5: Electromagnetic Torque (N.m).

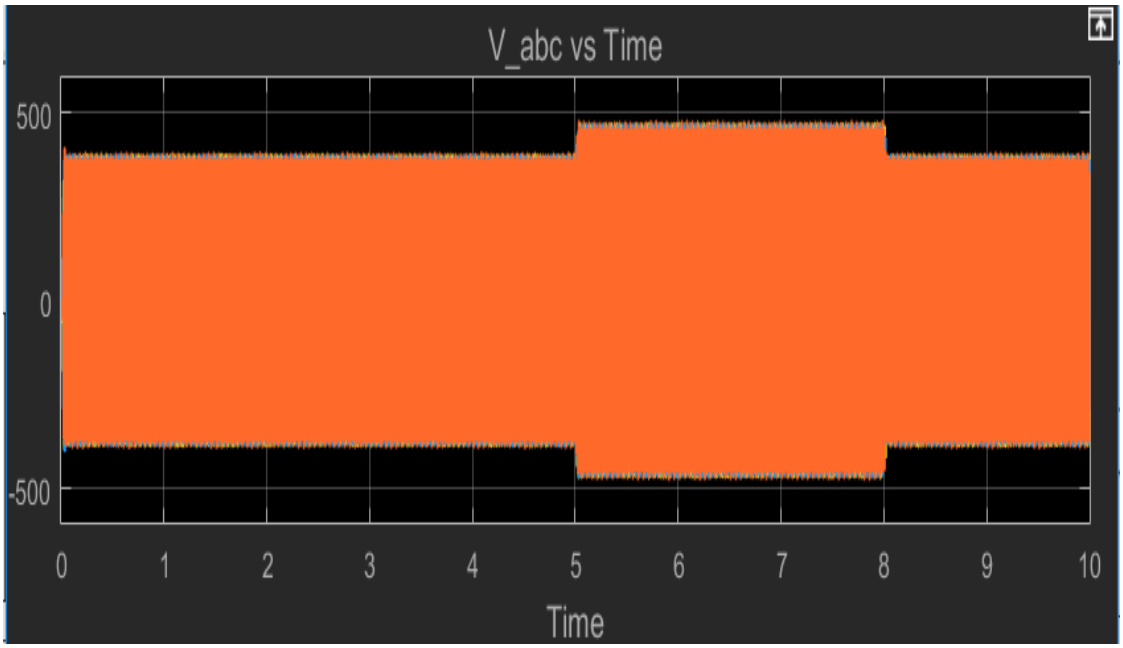

Figure 5.6: Three phase voltage at the load without VSG control (volts).

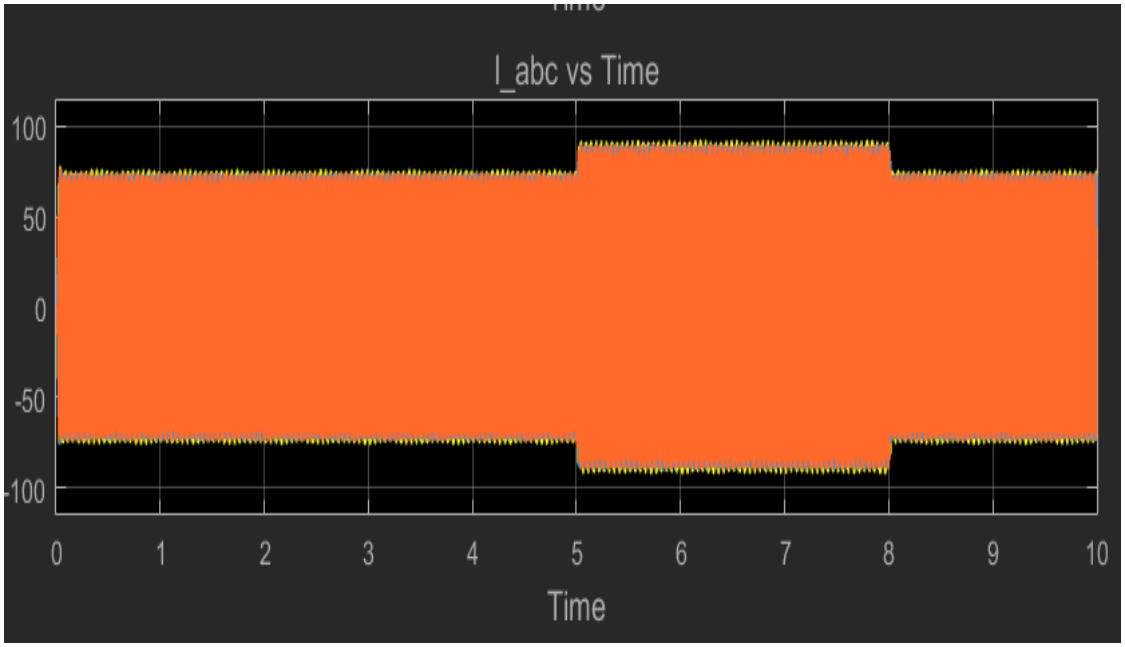

Figure 5.7: Three phase current at the load without VSG control (ampere).

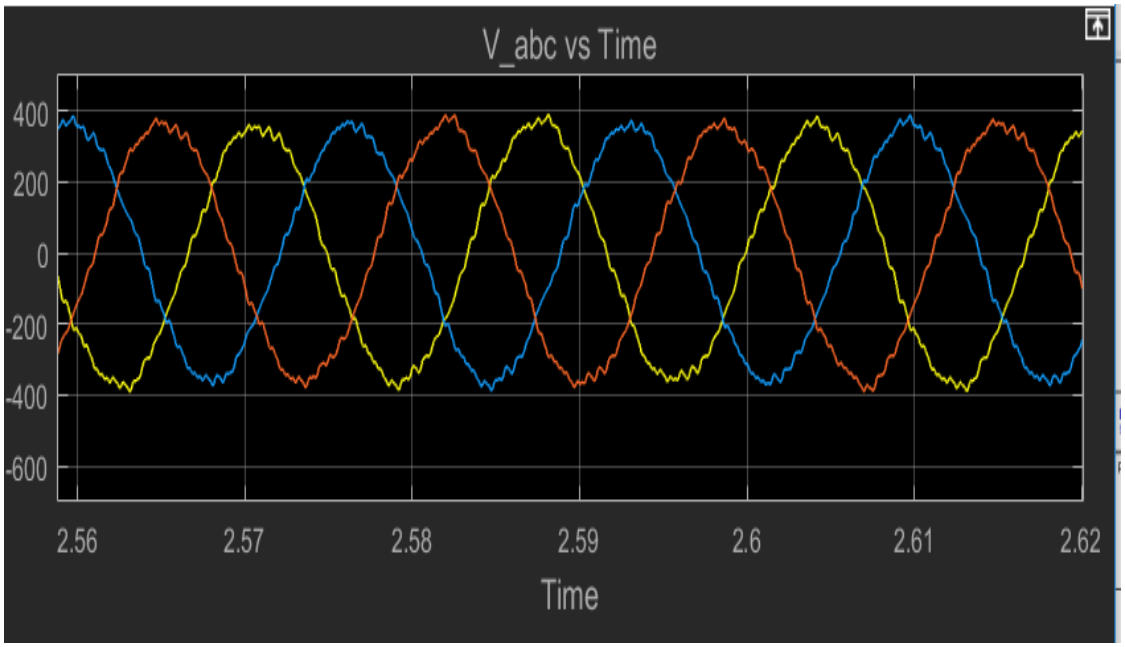

Figure 5.8: The three phase voltage zoom in graph (volts) .

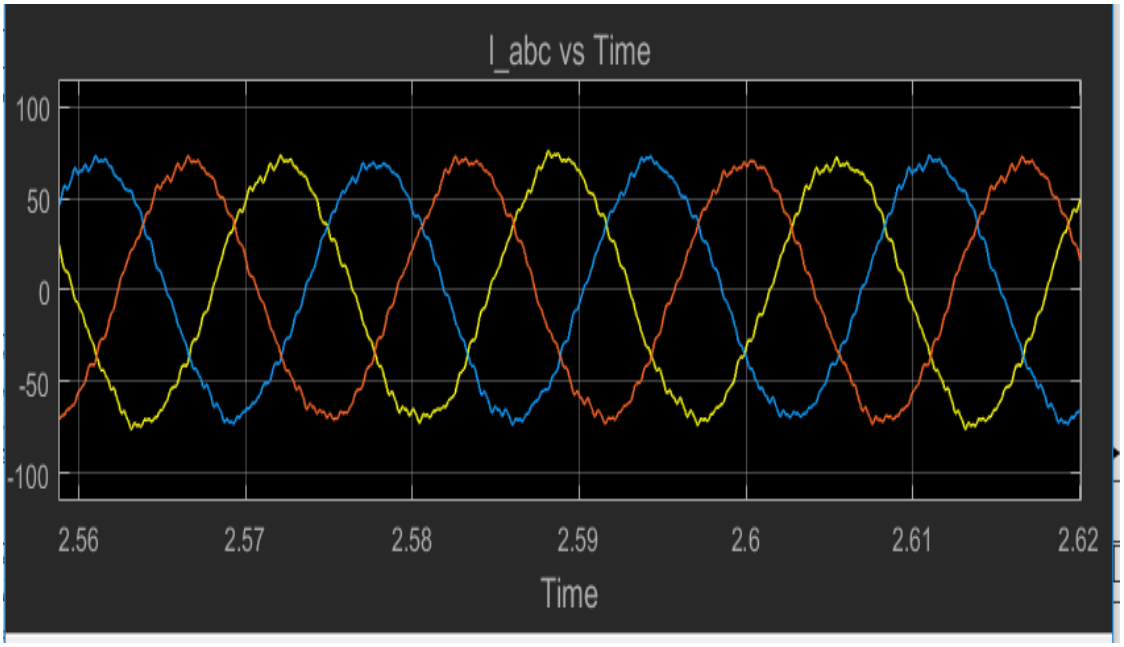

Figure 5.9: Three phase current zoom in graph (ampere).

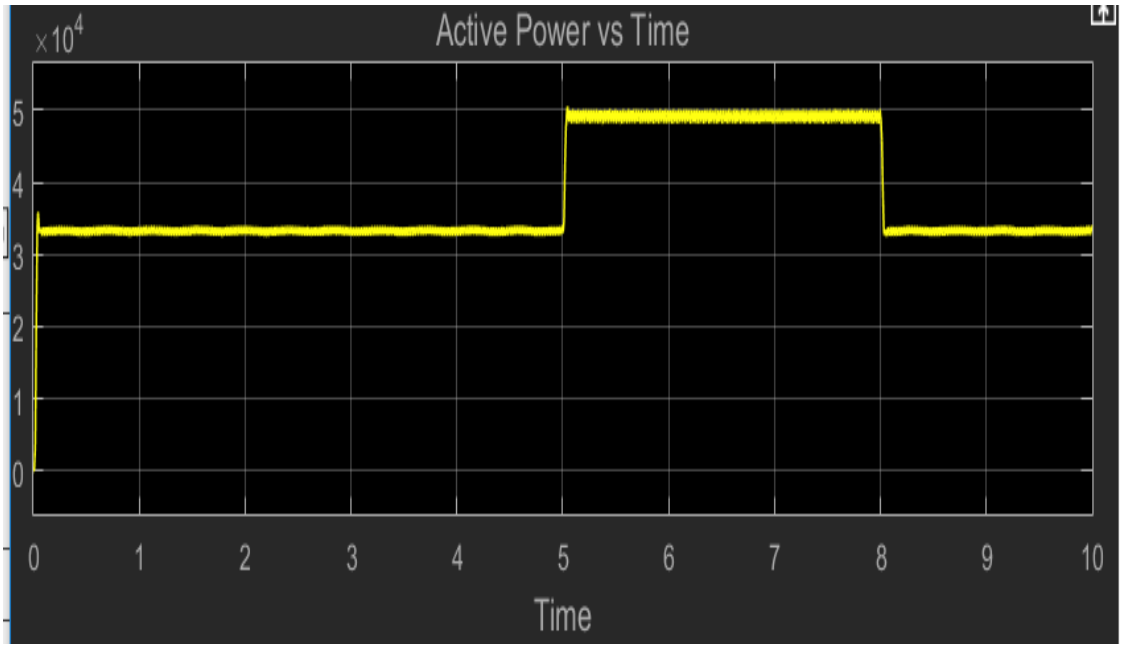

Figure 5.10: Active/Real Power without VSG control (10KWatts).

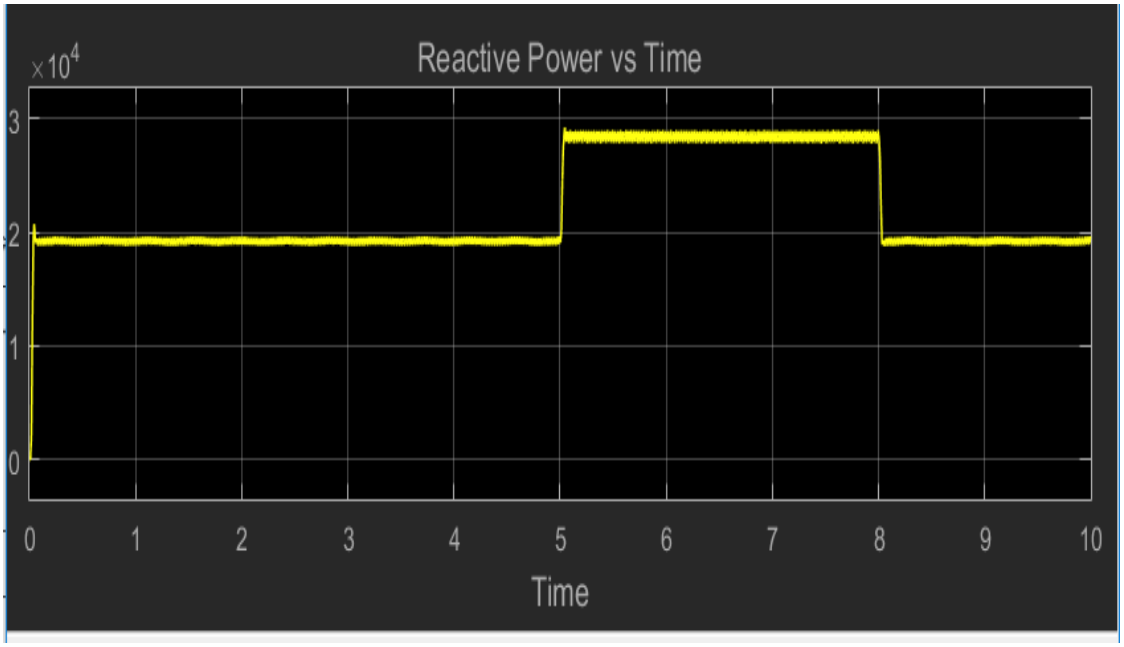

Figure 5.11: Reactive power without VSG control (10KVar).

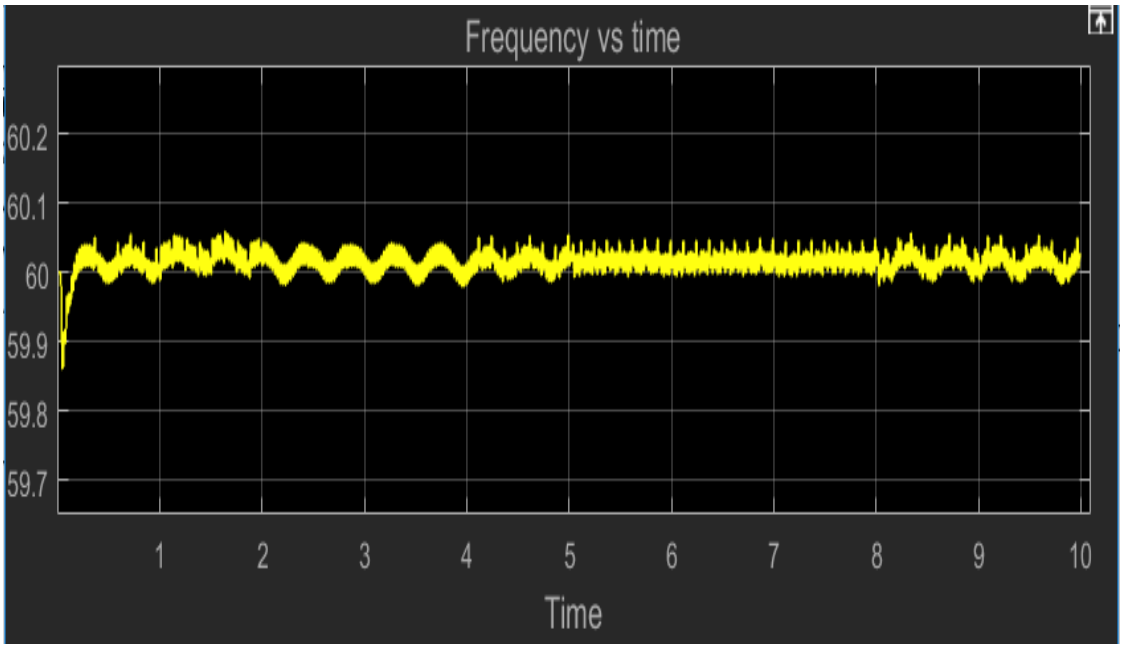

Figure 5.12: Frequency without VSG control (Hz).

The active and reactive power is shown in the figures 5.10 and 5.11 respectively. Power is increased when there is a increase in the wind speed with out maintaining the constant output. Figure 5.12 shows the frequency which is maintained at 60 Hz. This is because the PWM generator with 60Hz frequency and switching frequency 1600Hz is used to control the inverter. Here the frequency is maintained constant but not the output power. To maintain the output power also constant the VSG control is used.

The next case is the simulation results when there is a change in the input or other disturbances and system with VSG control and super capacitor. The overview of the system with VSG (controlled inverter) and super capacitor is shown in the figure 5.13.

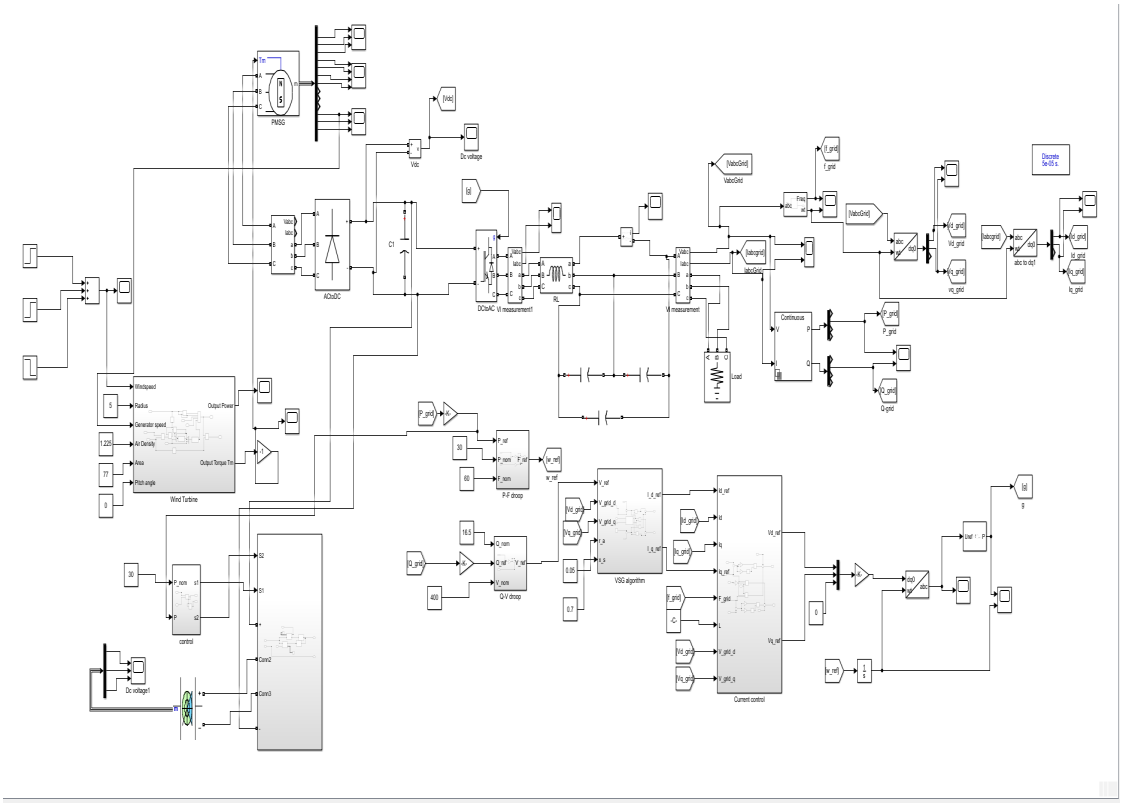

Figure 5.13: Overview of the Power system with VSG and supercapacitor.

The three phase voltage and current with VSG control are shown in the figures 5.14 and 5.15 respectively. From 5.14 and 5.15 it can shown that the output voltage and current are almost constant when there is a change in the wind speed. The dq components

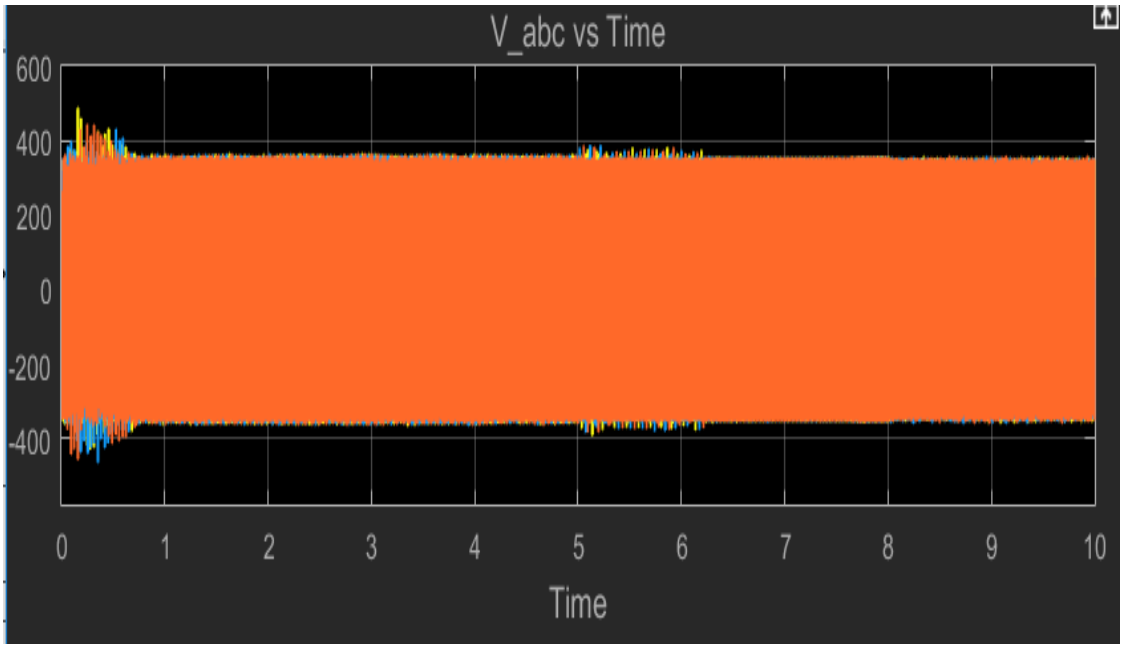

Figure 5.14: Three phase voltage with VSG (volts).

of the voltage and the current are shown in 5.17, 5.18 and 5.19, 5.20 respectively. The sine waves of the voltage and current are shown in the figures 5.21 and 5.22 respectively.

From the figure 5.23 and 5.25, it can be shown that, the output power is stable with the disturbances in the input by implementing VSG method to control the grid side inverter. The frequency of the grid is also maintained constant st 60Hz which is shown in figure 5.16. Figure 5.25 shows the charging and discharging of capacitor. In this thesis, the full rated voltage of the super capacitor is taken as 700V and the initial voltage is taken as 360V which is around 50 percent of the full rated voltage. When the wind speed is increased from 10m/s to 12m/s at time t= 5sec, there is a charging of the capacitor and at time t= 8sec the wins speed is decreased to 10m/s, it stops charging.

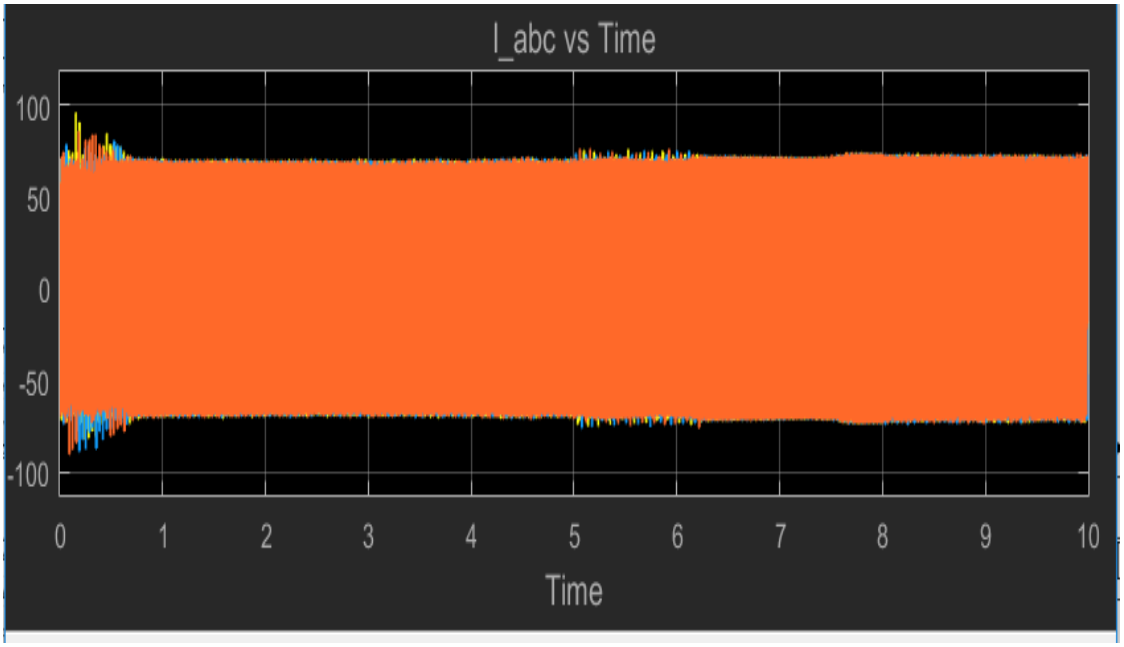

Figure 5.15: Three phase current with VSG (ampere).

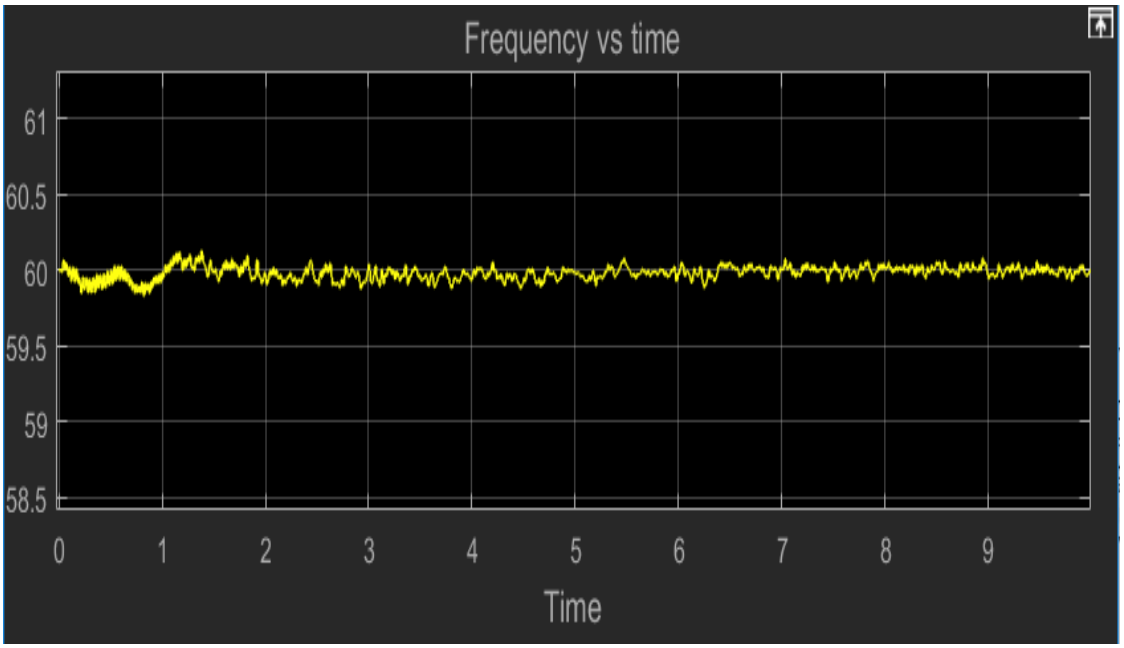

Figure 5.16: Frequency with VSG (Hz).

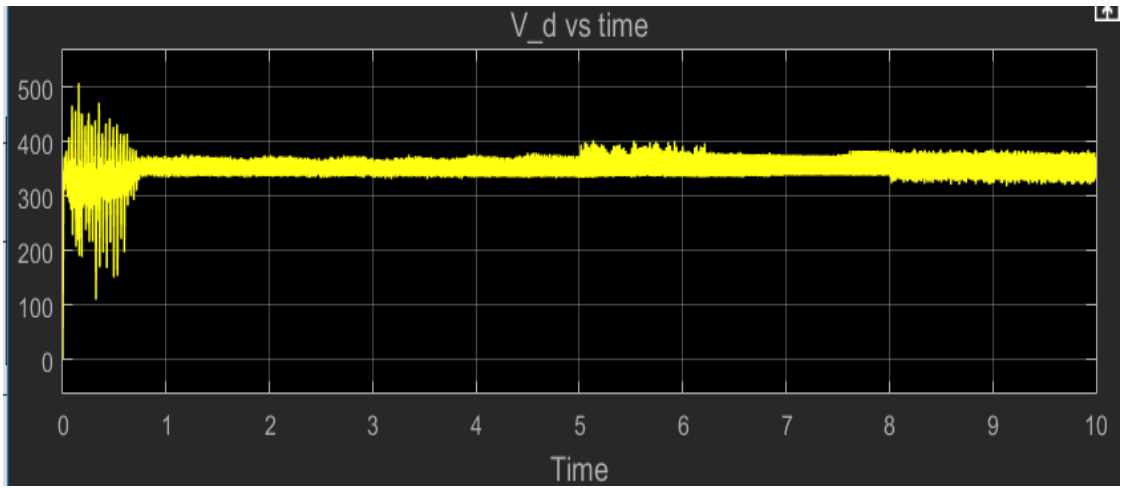

Figure 5.17: d-axis voltage with VSG (volts).

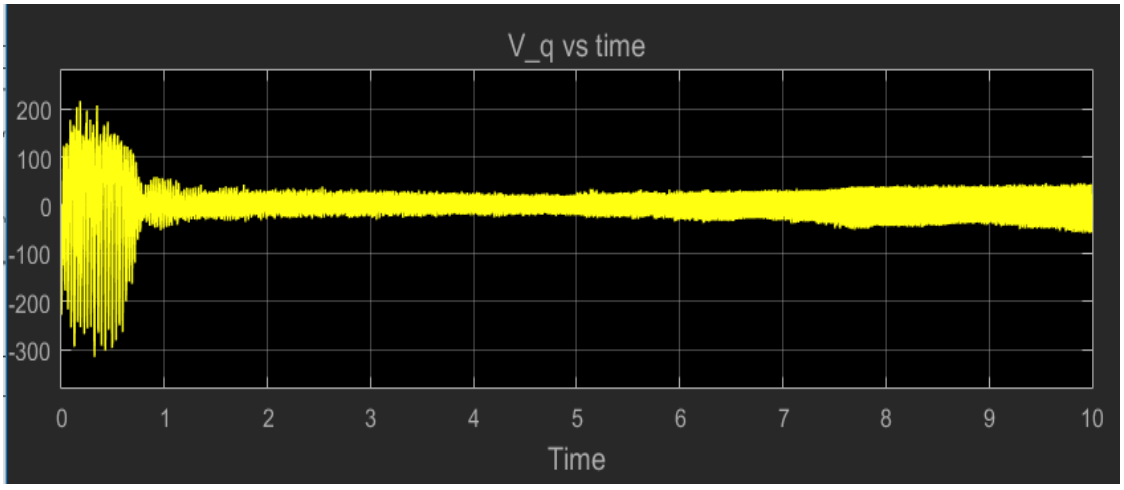

Figure 5.18: q-axis voltage with VSG (volts).

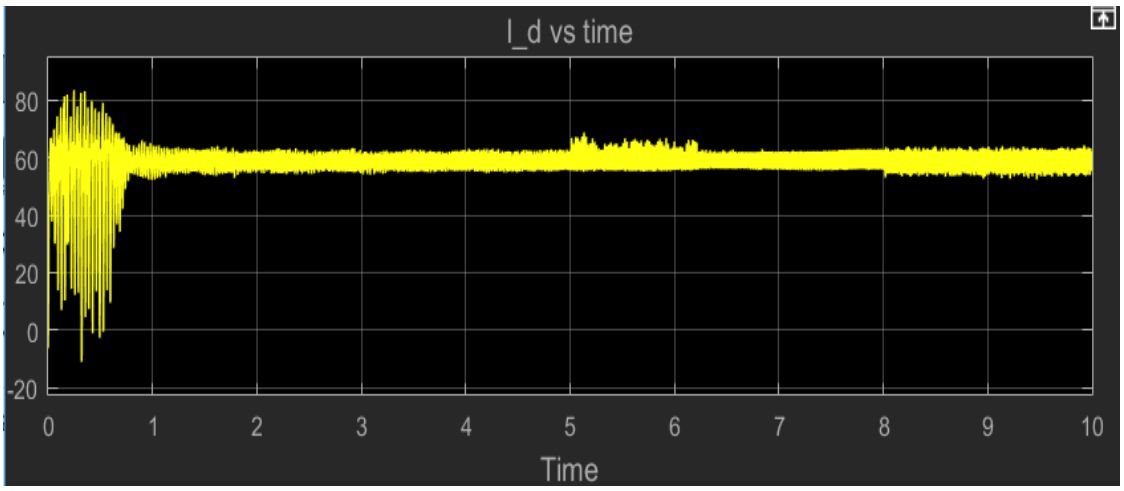

Figure 5.19: d-axis current with VSG (ampere).

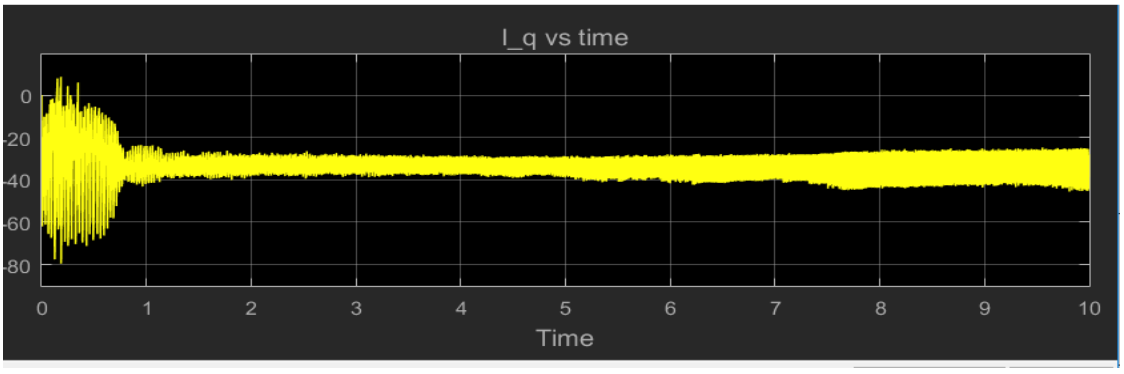

Figure 5.20: q-axis current with VSG (ampere).

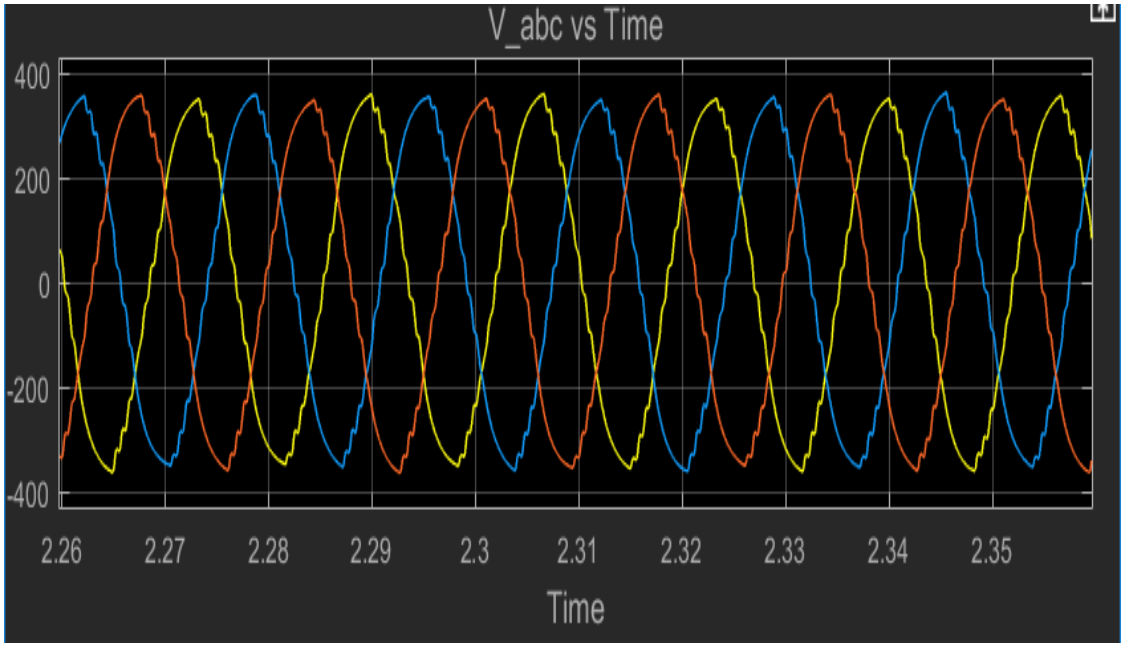

Figure 5.21: V_{abc} sine wave (volts).

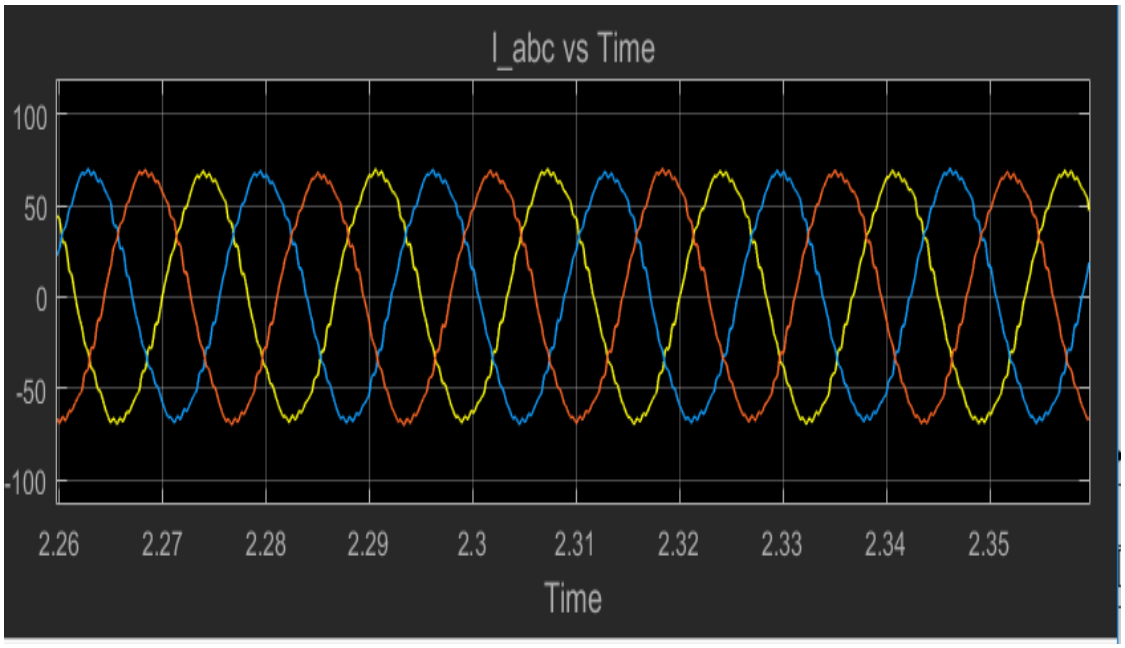

Figure 5.22: I_{abc} sine wave (ampere).

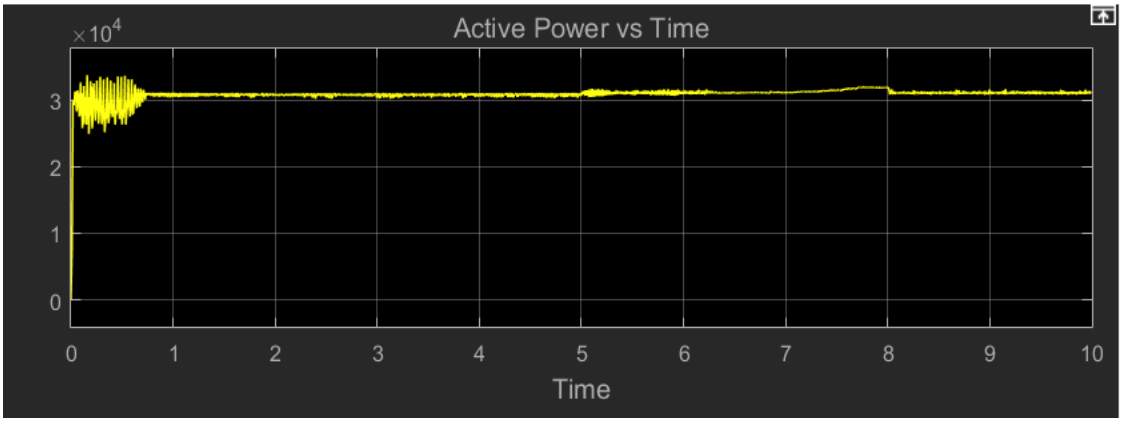

Figure 5.23: Active/Real power with VSG (10KWatts).

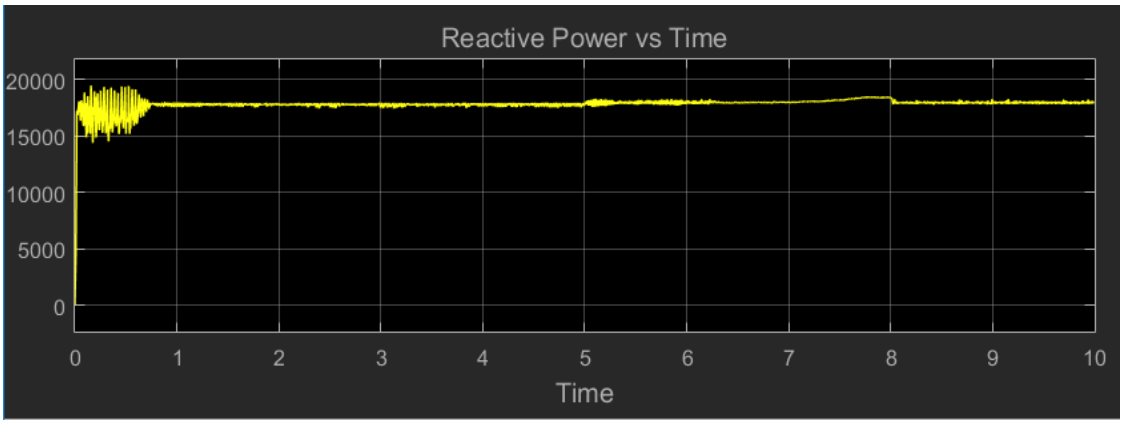

Figure 5.24: Reactive Power with VSG (10KVar).

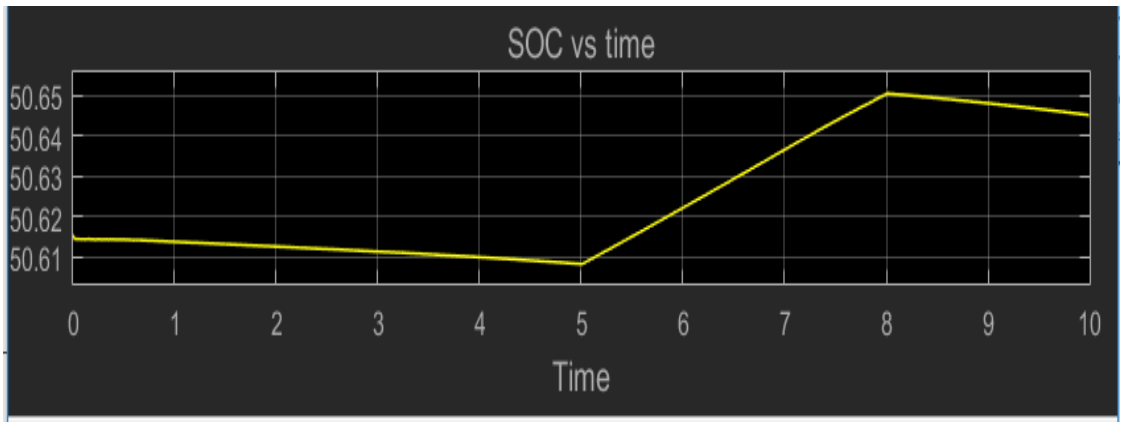

Figure 5.25: Charging and discharging of a capacitor (percentage).

Chapter 6

CONCLUSION AND FUTURE WORK

6.1 Conclusion

In this thesis, wind is modeled as the constant speed with fluctuations which led to the wind gust model. Then a wind turbine was modeled by using wind power equations and the AFPMSG is implemented. Since the direct integration of the Distributed Generators are not suitable for direct integration, there is a need to connect AC-DC and DC-AC converters to the AFPMSG. Because of the wind speed fluctuations, there are fluctuations in the output power and the frequency. To mitigate these issues, virtual synchronous generator was introduced. By using the VSG, the inverter is controlled in a way that it can function as the conventional synchronous generator.

The droop controllers ($P-F$ droop control and the $Q-V$ droop control) were introduced to generate the virtual inertia and damping properties. In this thesis, the islanded mode which supplies power to the load was used. The super capacitor is used to store the energy when there is a difference in the nominal power and the measured output power. SC is connected across the DC link of the power inverter. Simulation results of the WECS with variable wind speed was presented in chapter 5.

6.2 Future Work

In this research, islanded micro grid mode which inverter is connected to the load is used. This must be extended for grid connected which means inverter is connected to the grid.In the current control model of the VSG, K_p and K_I constants were chosen by trial and error method. This causes the oscillations in power and frequency in the beginning. To prevent these fluctuations in the beginning, these constants must be determined by using a mathematical model. The VSG control model is more complex. Improvement of computing techniques and improvement of modeling will reduce the VSG structure complexity.

References

[1] S. Sawyer and K. Rave, "Gwec–global wind report| annual market update 2014," 2014.

[2] U. D. of Energy Report, "Current installed wind power capacity," 02-Feb-2017.

[3] K. Sakimoto, Y. Miura, and T. Ise, "Stabilization of a power system with a distributed generator by a virtual synchronous generator function," in *Power Electronics and ECCE Asia (ICPE & ECCE), 2011 IEEE 8th International Conference on*. IEEE, 2011, pp. 1498–1505.

[4] O. Edenhofer, R. Pichs-Madruga, Y. Sokona, K. Seyboth, P. Matschoss, S. Kadner, T. Zwickel, P. Eickemeier, G. Hansen, S. Schlömer *et al.*, "Ipcc special report on renewable energy sources and climate change mitigation," *Prepared By Working Group III of the Intergovernmental Panel on Climate Change, Cambridge University Press, Cambridge, UK*, 2011.

[5] S. Muyeen, R. Takahashi, T. Murata, and J. Tamura, "A variable speed wind turbine control strategy to meet wind farm grid code requirements," *IEEE Transactions on power systems*, vol. 25, no. 1, pp. 331–340, 2010.

[6] A. A. Pop, F. Jurca, C. Oprea, M. Chirca, S. Breban, and M. M. Radulescu, "Axial-flux vs. radial-flux permanent-magnet synchronous generators for micro-wind turbine application," in *Power Electronics and Applications (EPE), 2013 15th European Conference on*. IEEE, 2013, pp. 1–10.

[7] V. Akhmatov, "Analysis of dynamic behavior of electric power systems with large amount of wind power," *Electrical Power Engineering*, 2003.

[8] R. Datta and V. Ranganathan, "Variable-speed wind power generation using doubly fed wound rotor induction machine-a comparison with alternative schemes," *IEEE transactions on Energy conversion*, vol. 17, no. 3, pp. 414–421, 2002.

[9] X. Yuan, Y. Li, J. Chai, and M. Ma, "A modular direct-drive permanent magnet wind generator system eliminating the grid-side transformer," in *Power Electronics and Applications, 2009. EPE'09. 13th European Conference on*. IEEE, 2009, pp. 1–7.

[10] S. Zhang, K.-J. Tseng, D. M. Vilathgamuwa, T. D. Nguyen, and X.-Y. Wang, "Design of a robust grid interface system for pmsg-based wind turbine generators," *IEEE transactions on industrial electronics*, vol. 58, no. 1, pp. 316–328, 2011.

[11] R. K. Gupta, G. F. Castelino, K. K. Mohapatra, and N. Mohan, "A novel integrated three-phase, switched multi-winding power electronic transformer converter for wind power generation system," in *Industrial Electronics, 2009. IECON'09. 35th Annual Conference of IEEE*. IEEE, 2009, pp. 4481–4486.

[12] M. Yin, G. Li, M. Zhou, and C. Zhao, "Modeling of the wind turbine with a permanent magnet synchronous generator for integration," in *Power Engineering Society General Meeting, 2007. IEEE*. IEEE, 2007, pp. 1–6.

[13] S. Venkatraj and G. Mohan, "Modeling of wind farms with variable speed direct driven permanent magnet synchronous generator wind turbines," *International Journal of Research and Reviews in Electrical and Computer Engineering*, vol. 1, no. 3, pp. 982–990, 2011.

[14] A. Rolan, A. Luna, G. Vazquez, D. Aguilar, and G. Azevedo, "Modeling of a variable speed wind turbine with a permanent magnet synchronous generator," in *Industrial Electronics, 2009. ISIE 2009. IEEE International Symposium on*. IEEE, 2009, pp. 734–739.

[15] B. Mangu, S. Akshatha, D. Suryanarayana, and B. Fernandes, "Grid-connected pv-wind-battery-based multi-input transformer-coupled bidirectional dc-dc converter

for household applications," *IEEE journal of emerging and selected topics in power electronics*, vol. 4, no. 3, pp. 1086–1095, 2016.

[16] H. Bevrani, T. Ise, and Y. Miura, "Virtual synchronous generators: A survey and new perspectives," *International Journal of Electrical Power & Energy Systems*, vol. 54, pp. 244–254, 2014.

[17] T. Loix, S. De Breucker, P. Vanassche, J. Van den Keybus, J. Driesen, and K. Visscher, "Layout and performance of the power electronic converter platform for the vsync project," in *PowerTech, 2009 IEEE Bucharest*. IEEE, 2009, pp. 1–8.

[18] K. Visscher and S. W. H. De Haan, "Virtual synchronous machines (vsg's) for frequency stabilisation in future grids with a significant share of decentralized generation," in *SmartGrids for Distribution, 2008. IET-CIRED. CIRED Seminar*. IET, 2008, pp. 1–4.

[19] Y. Chen, R. Hesse, D. Turschner, and H.-P. Beck, "Comparison of methods for implementing virtual synchronous machine on inverters," in *International Conference on Renewable Energies and Power Quality*, 2012, pp. 1–6.

[20] ——, "Improving the grid power quality using virtual synchronous machines," in *Power engineering, energy and electrical drives (POWERENG), 2011 international conference on*. IEEE, 2011, pp. 1–6.

[21] Y. Hirase, K. Abe, K. Sugimoto, and Y. Shindo, "A grid-connected inverter with virtual synchronous generator model of algebraic type," *Electrical Engineering in Japan*, vol. 184, no. 4, pp. 10–21, 2013.

[22] T. Shintai, Y. Miura, and T. Ise, "Reactive power control for load sharing with virtual synchronous generator control," in *Power Electronics and Motion Control Conference (IPEMC), 2012 7th International*, vol. 2. IEEE, 2012, pp. 846–853.

[23] Q.-C. Zhong and G. Weiss, "Synchronverters: Inverters that mimic synchronous generators," *IEEE Transactions on Industrial Electronics*, vol. 58, no. 4, pp. 1259–1267, 2011.

[24] G. Elert, "The physics hypertextbook," *Found July*, vol. 9, p. 2008, 1998.

[25] M. Ragheb, "Wind energy conversion theory, betz equation," *Wind Energie*, 2014.

[26] Z. Salameh, "Modeling and simulation of a wind turbine-generator system," in *Power and Energy Society General Meeting, 2011 IEEE*. IEEE, 2011, pp. 1–7.

[27] A. Betz, "Behavior of vortex systems," 1933.

[28] T. Sun, Z. Chen, and F. Blaabjerg, "Voltage recovery of grid-connected wind turbines after a short-circuit fault," in *Industrial Electronics Society, 2003. IECON'03. The 29th Annual Conference of the IEEE*, vol. 3. IEEE, 2003, pp. 2723–2728.

[29] J. Salazar, F. Tadeo, C. de Prada, and L. Palacin, "Modeling and control of a wind turbine equipped with a permanent magnet synchronous generator (pmsg)," in *Proc. of the 22nd European Modeling & Simulation Symposium*, 2010, pp. 13–15.

[30] N. Huang, "Simulation of power control of a wind turbine permanent magnet synchronous generator system," 2013.

[31] S. Crary, "Two-reaction theory of synchronous machines," *Transactions of the American Institute of Electrical Engineers*, vol. 56, no. 1, pp. 27–36, 1937.

[32] E. Adzic, V. Porobic, B. Dumnic, N. Celanovic, and V. Katic, "Pll synchronization in grid-connected converters," in *The 6th PSU-UNS International Conference on Engineering and Technology (ICET-2013)*, 2013, pp. 1–5.

[33] S.-J. Ahn, J.-W. Park, I.-Y. Chung, S.-I. Moon, S.-H. Kang, and S.-R. Nam, "Power-sharing method of multiple distributed generators considering control modes and configurations of a microgrid," *IEEE Transactions on Power Delivery*, vol. 25, no. 3, pp. 2007–2016, 2010.

[34] M. A. Islam, "Implementation of virtual synchronous generator methodologies for renewable integration," Ph.D. dissertation, Temple University, 2017.

[35] A. Perera, "Virtual synchronous machine-based power control in active rectifiers for micro grids," Master's thesis, Institutt for elkraftteknikk, 2012.

[36] A. Naderipour, A. A. M. Zin, M. H. B. Habibuddin, M. R. Miveh, and J. M. Guerrero, “An improved synchronous reference frame current control strategy for a photovoltaic grid-connected inverter under unbalanced and nonlinear load conditions,” *PloS one*, vol. 12, no. 2, p. e0164856, 2017.